



# Dereplication of Acetogenins from *Annona muricata* by Combining Tandem Mass Spectrometry after Lithium and Copper Postcolumn Cationization and Molecular Networks

Salomé Poyer, Laurent Laboureur, Téo Hebra, Nicolas Elie, Guillaume van Der Rest, Jean-Yves Salpin, Pierre Champy, David Touboul

## ► To cite this version:

Salomé Poyer, Laurent Laboureur, Téo Hebra, Nicolas Elie, Guillaume van Der Rest, et al.. Dereplication of Acetogenins from *Annona muricata* by Combining Tandem Mass Spectrometry after Lithium and Copper Postcolumn Cationization and Molecular Networks. *Journal of The American Society for Mass Spectrometry*, 2022, 33 (4), pp.627-634. 10.1021/jasms.1c00303 . hal-03780186

HAL Id: hal-03780186

<https://hal.science/hal-03780186v1>

Submitted on 19 Sep 2022

**HAL** is a multi-disciplinary open access archive for the deposit and dissemination of scientific research documents, whether they are published or not. The documents may come from teaching and research institutions in France or abroad, or from public or private research centers.

L'archive ouverte pluridisciplinaire **HAL**, est destinée au dépôt et à la diffusion de documents scientifiques de niveau recherche, publiés ou non, émanant des établissements d'enseignement et de recherche français ou étrangers, des laboratoires publics ou privés.

# **Dereplication of acetogenins from *Annona muricata* by combining tandem mass spectrometry after lithium and copper post-column cationization and molecular networks**

Salomé Poyer,<sup>1\*</sup> Laurent Laboureur,<sup>1</sup> Téo Hebra,<sup>1</sup> Nicolas Elie,<sup>1</sup> Guillaume Van der Rest,<sup>2</sup> Jean-Yves Salpin,<sup>3,4</sup> Pierre Champy,<sup>5</sup> David Touboul<sup>1\*</sup>

1. Université Paris-Saclay, CNRS, Institut de Chimie des Substances Naturelles, UPR 2301, 91198, Gif-sur-Yvette, France.
2. Université Paris-Saclay, CNRS, Institut de Chimie Physique, 91405, Orsay, France.
3. Université Paris-Saclay, Univ Evry, CNRS, LAMBE, 91025, Evry-Courcouronnes, France.
4. LAMBE, CY Cergy Paris Université, CNRS, 95000 Cergy, France.
5. Université Paris-Saclay, CNRS, BioCIS, 92290, Châtenay-Malabry, France.

## **Supporting Information**

The Supporting Information is available free of charge on the ACS Publications website.

## **Author Information**

### **Corresponding Authors**

\* [Salome.poyer@gmail.com](mailto:Salome.poyer@gmail.com)

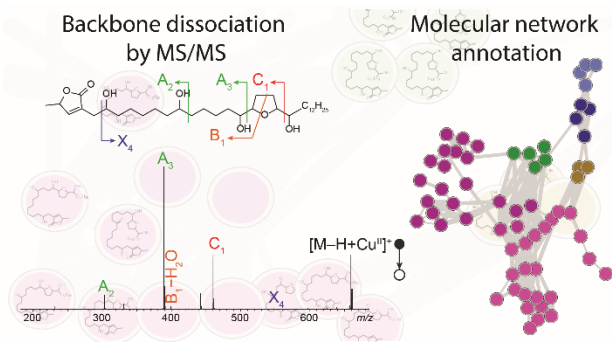
\* [David.touboul@cnrs.fr](mailto:David.touboul@cnrs.fr)

### **Author Contributions**

The manuscript was written through contributions of all authors. All authors have given approval to the final version of the manuscript.

## Abstract

Annonaceous acetogenins are natural products held responsible for atypical parkinsonism due to chronic consumption in traditional medicine or as food. Due to their long-term neurotoxic effects in humans, the complete chemical characterization of acetogenins in complex mixtures has become crucial. Characterization by tandem mass spectrometry (MS/MS) of acetogenins using collision-induced dissociation (CID) from lithium adducts provides additional structural information compared to protonated or sodiated species such as ketone location on the acetogenins backbone. However, diagnostic ions are present at a very low intensity limiting this approach to abundant species in the extracts. Copper adducts led to diagnostic fragment ions that allow to identify the position of oxygen rings and hydroxyl substituents. Fragmentation rules were established based on acetogenin standards allowing the identification of 45 over the 77 analogues observed in an extract of *Annona muricata* by LC-MS/MS using post-column infusion of copper sulfate ( $\text{CuSO}_4$ ) solution. Molecular networks that were generated thanks to specific fragmentations obtained with copper, led to the distinction of THF ring position or to the identification of hydroxylated lactone for instance, while networks generated from lithium adducts mainly distinguish analogues with a hydroxyl group at C<sub>4</sub> from the other structures.



## Introduction

Annonaceous acetogenins are present at a millimolar level in tropical plants from *Annona* genus.<sup>1</sup>,<sup>2</sup> Their various biological properties, both detrimental and beneficial, along with their widespread consumption, particularly as fruits, make their characterization an urgent need.<sup>3</sup> The accurate structural characterization of acetogenins is difficult because of their long carbon chains. Acetogenins consist of 35 or 37 carbon atoms bearing a terminal  $\gamma$ -methyl- $\gamma$ -lactone. They are constituted of an alkyl chain with oxygen-containing substituent and a central oxygen ring domain with motifs such as tetrahydrofurans, tetrahydropyrans or epoxides flanked or not by hydroxyl groups. More than 530 analogues have been reported in the literature.<sup>4</sup> The NMR characterization of these analogues is difficult due to the length of the alkyl chains, allowing the determination of the chemical functions but not their complete localization on the molecule. Moreover, NMR identification requires the isolation of each compound and does not allow dereplication of complex mixtures as opposed to liquid chromatography – mass spectrometry (LC-MS).

Tandem mass spectrometry (MS/MS) of protonated acetogenins leads mainly to losses of H<sub>2</sub>O, which do not provide any structural information.<sup>5</sup> It has been shown that collision induced dissociation (CID) of the lithiated adducts improves the quality of structural information.<sup>5-7</sup> LC<sup>8</sup>,<sup>9</sup> and supercritical fluid chromatography (SFC)<sup>10</sup> coupled to MS/MS experiments with post-column infusion of a lithium salt in solution have made possible the partial characterization of acetogenins present in complex natural extracts. However, the structurally informative fragments are observed in low abundance and a lack of information remains for substitution further than four carbons from the lactone function.

The use of copper adducts in CID MS/MS allowed in specific cases dissociation of strong chemical bonds such as C-C of aliphatic chains<sup>11</sup> or pyran rings.<sup>12</sup> In fact, Cu<sup>II+</sup> can easily be reduced under low energy collisional conditions to reach a complete d<sup>10</sup> shell, yielding a free radical. The delocalization of the electron will result in the cleavage of stronger bonds than in non-radical induced CID processes.<sup>13</sup>

The fragmentation pathways of copper-cationized acetogenins were investigated by CID experiments from standard analogues. The main fragmentation pathways were putatively supported by gas-phase reactions, and the MS<sup>n</sup> results on [M–H+Cu<sup>II</sup>]<sup>+</sup> ions were compared to

lithium adducts. Molecular networks (MN) for either Cu<sup>2+</sup> and Li<sup>+</sup> cationized species were employed to guide the identification of 45 acetogenins in a seed extract of *Annona muricata*.

## Experimental part

### ***Chemicals***

Copper sulfate, lithium iodide and sodium formate were purchased from Sigma-Aldrich (Sigma-Aldrich, Saint Quentin-Fallavier, France). Methanol (MeOH) and acetonitrile (MeCN) LCMS grade were purchased from VWR-Prolabo (Fontenay-sous-Bois, France). Deionised water (18.2 MΩ) was obtained from a Milli-Q apparatus (Saint-Quentin-Yvelines, France). Annonacin (C<sub>35</sub>H<sub>64</sub>O<sub>7</sub>), annonacinone (C<sub>35</sub>H<sub>62</sub>O<sub>7</sub>), squamocin (C<sub>37</sub>H<sub>66</sub>O<sub>7</sub>), rolliniastatin-1 (C<sub>37</sub>H<sub>66</sub>O<sub>7</sub>), desacetyl-uvaricin (C<sub>37</sub>H<sub>66</sub>O<sub>6</sub>), diepomuricanin-A (C<sub>35</sub>H<sub>62</sub>O<sub>4</sub>), montecristin (C<sub>37</sub>H<sub>66</sub>O<sub>4</sub>) and seeds extract of *Annona muricata* were obtained as previously described.<sup>1, 10</sup> Stock solutions were prepared in methanol at a concentration of 100 µg/mL.

### ***MS<sup>n</sup> experiments***

MS<sup>n</sup> experiments were performed using a LTQ-XL-Orbitrap (Thermo Scientific, Les Ulis, France) equipped with an electrospray (ESI) source operated in the positive ionization mode. Ion source conditions were set as follows: source voltage 4 kV, capillary voltage 20 V, tube lens voltage 120 V, sheath gas flow rate 5 arbitrary unit and capillary temperature 275 °C. The mass spectrometer was calibrated for a resolution of 30 000 using the commercial tune mix. Standards diluted at 10 µg/mL in a methanolic solution containing 100 µM of CuSO<sub>4</sub> or LiI were infused at 10 µL/min. Thermo Xcalibur software v2.2 was used to process MS<sup>n</sup> data.

### ***LC-IMS-MS/MS experiments***

Liquid chromatography – tandem mass spectrometry (LC-MS/MS) experiments were performed on an Acquity I-Class LC system coupled to a Synapt G2-Si mass spectrometer (Waters, Manchester, UK) equipped with an ESI source operated in the positive ionization mode. The chromatographic separation was carried out on a Ascentis Express C<sub>18</sub> (150 × 2.1 mm, 2.7 µM)

column heated at 50 °C at a flow rate of 550 µL/min with water as solvent A and acetonitrile as solvent B. 5 µL of *Annona muricata* extract at 10 mg/mL in MeOH (due to lower solubility in MeCN/water) were injected using the following gradient: 0 min (65% B), 5 min (65% B), 25 min (85% B), 26 min (100% B), 30 min (100% B), 31 min (65% B), and 4 min of equilibration time. A 10 µL/min post-column infusion of CuSO<sub>4</sub> or LiI in MeOH at 1 µM or 10 µM, respectively, was performed downstream of a 1:10 split flow rate using a syringe pump. Ion source conditions were set as follows: capillary voltage 3 kV, sampling cone voltage 40 V, source offset voltage 80 V, source temperature 80 °C, desolvation gas temperature 150 °C at a flow rate of 100 L/h. IMS conditions were also set as follows: helium gas flow 180 mL/min, IMS (N<sub>2</sub>) gas flow 50 mL/min, wave velocity 500 m/s and wave height 25 V. The TOF was daily calibrated in the 50-1200 *m/z* mass range in “V resolution” mode using a sodium formate solution. Masslynx v4.1 and Driftscope v2.7 software were used to process data.

### ***Molecular network generation***

Molecular networks were generated with the MetGem software from LC-MS/MS data using targeted mode on *Annona muricata* extracts.<sup>14</sup> IMS dimension was not taken into account to generate the molecular networks, but only used to manually distinguish isobaric species. MS/MS spectra were centroided and calibrated from the precursor ion as internal standard before extraction using MZmine 2.52<sup>15</sup> using the following parameters: mass detection noise level 50; ADAP chromatogram builder group intensity threshold 600, min highest intensity 300, *m/z* tolerance 0.005 *m/z* or 20 ppm; chromatogram deconvolution wavelets, S/N threshold 3, min feature height 10, peak duration range 0.00–2.00 min, tr wavelet range 0.00–0.08, *m/z* range for MS/MS scan pairing 0.5, tr range for MS/MS scan pairing 0.5. Molecular networks parameters of MetGem 1.3.4 were a minimum of 2 matched fragment ions and a cosine score of 0.7 after the filtering of peaks at ± 17 Da from the precursor ion for Cu and ± 14 Da or 100 Da for Li and keeping all fragment ions above 1%. In fact, lithium adducted acetogenins yield mainly non-structural informative fragments such as water losses that give high cosine scores while the first informative fragment is the lactone loss (X) at 112 Da from the precursor lithiated ion (Figure S20). Since all uninformative fragments are losses of neutrals less than 100 Da cumulative (H<sub>2</sub>O and CO<sub>2</sub> losses), we decided to remove these fragments from the cosine score calculation by increasing the peak filtering range around the precursor ions.

## Results and discussions

### *MS/MS of copper-cationized acetogenin standards*

The fragmentation of copper-adducted acetogenins CID was first tested with annonacin.<sup>16</sup> This molecule is composed of a  $\gamma$ -methyl- $\gamma$ -lactone substituted by an alkyl chain on C<sub>2</sub>, hydroxyl substituents in C<sub>4</sub>, C<sub>10</sub>, C<sub>15</sub> and C<sub>20</sub>, and a single THF between the two latter hydroxyl functions.<sup>17</sup> The MS/MS spectrum of protonated annonacin only exhibits losses of water (Figure S1). Its structural characterization can be achieved from lithium-cationized species through the detection of a series of X and B fragments (Figure 1a).<sup>5,8</sup>

The MS analysis of annonacin in solution with CuSO<sub>4</sub> showed copper-containing ions in addition to protonated and sodiated species (Figure S2). We observed doubly charged species, such as [Annonacin+Cu<sup>II</sup>]<sup>2+</sup> and the dimer [2(Annonacin)+Cu<sup>II</sup>]<sup>2+</sup>, both also being observed as aggregates with CuSO<sub>4</sub>. The [Annonacin+Cu<sup>I</sup>]<sup>+</sup> ion resulting from copper reduction is also observed under cone voltages higher than 60 V and capillary voltages higher than 4 kV.<sup>11</sup> The dissociation of these species exhibited the loss of water as main dissociation pathway (data not shown). In addition, [Annonacin-H+Cu<sup>II</sup>]<sup>+</sup> ion was observed at lower ESI conditions, as described in the experimental part (Figure S2).

The dissociation of [Annonacin-H+Cu<sup>II</sup>]<sup>+</sup> ion yields intense copper containing fragments with odd *m/z* values suggesting Cu<sup>II</sup> reduction, except for ions at *m/z* 460.1869 and the successive loss of water at *m/z* 442.1765 which have either a radical [R<sup>•</sup>+Cu<sup>I</sup>]<sup>+</sup> or an unreduced F fragment (odd masses) [F<sup>-</sup>+Cu<sup>II</sup>]<sup>+</sup> form. The two main fragments, namely A<sub>3</sub> and C<sub>1</sub> according to the nomenclature established by Laprévote *et al.*,<sup>7</sup> contain the  $\gamma$ -methyl- $\gamma$ -lactone side of the molecule and were attributed to the cleavage of the C-C bond on each side of the THF group located between C<sub>16</sub> and C<sub>19</sub> atoms (Figure 1b). The location of the dihydroxylated THF was also supported by the presence of the B<sub>1</sub>-H<sub>2</sub>O fragment resulting from the THF opening.<sup>12</sup> Alpha-cleavage at the hydroxyl group on C<sub>10</sub> yields fragments A<sub>2</sub> and X<sub>3</sub> containing the hydroxyl moiety and the  $\gamma$ -methyl- $\gamma$ -lactone side or the alkyl chain end, respectively. The last hydroxyl function on the C<sub>4</sub> is characterized by the presence of the X<sub>4</sub> and Z<sub>4</sub> fragment ions at *m/z* 547.3406 and *m/z* 518.3367. Finally, two internal fragments were observed, corresponding to the C-C bond cleavage in alpha of the hydroxyl groups at C<sub>4</sub> or C<sub>10</sub> and a loss of H<sub>2</sub>O from the C<sub>1</sub> fragment ion. Based on MS<sup>2</sup> to

MS<sup>4</sup> results, the complete fragmentation pathway of the [Annonacin–H+Cu<sup>II</sup>]<sup>+</sup> ion was provided. It is important to note that the [Annonacin+Cu<sup>I</sup>]<sup>+</sup> ion was detected by using an isolation window of 2 Da due to the poor transmission of the [Annonacin–H+Cu<sup>II</sup>]<sup>+</sup> ion, and the gas-phase stability of [Annonacin+Cu<sup>I</sup>]<sup>+</sup> ion, higher than that of the [Annonacin–H+Cu<sup>II</sup>]<sup>+</sup> ion.<sup>11</sup>

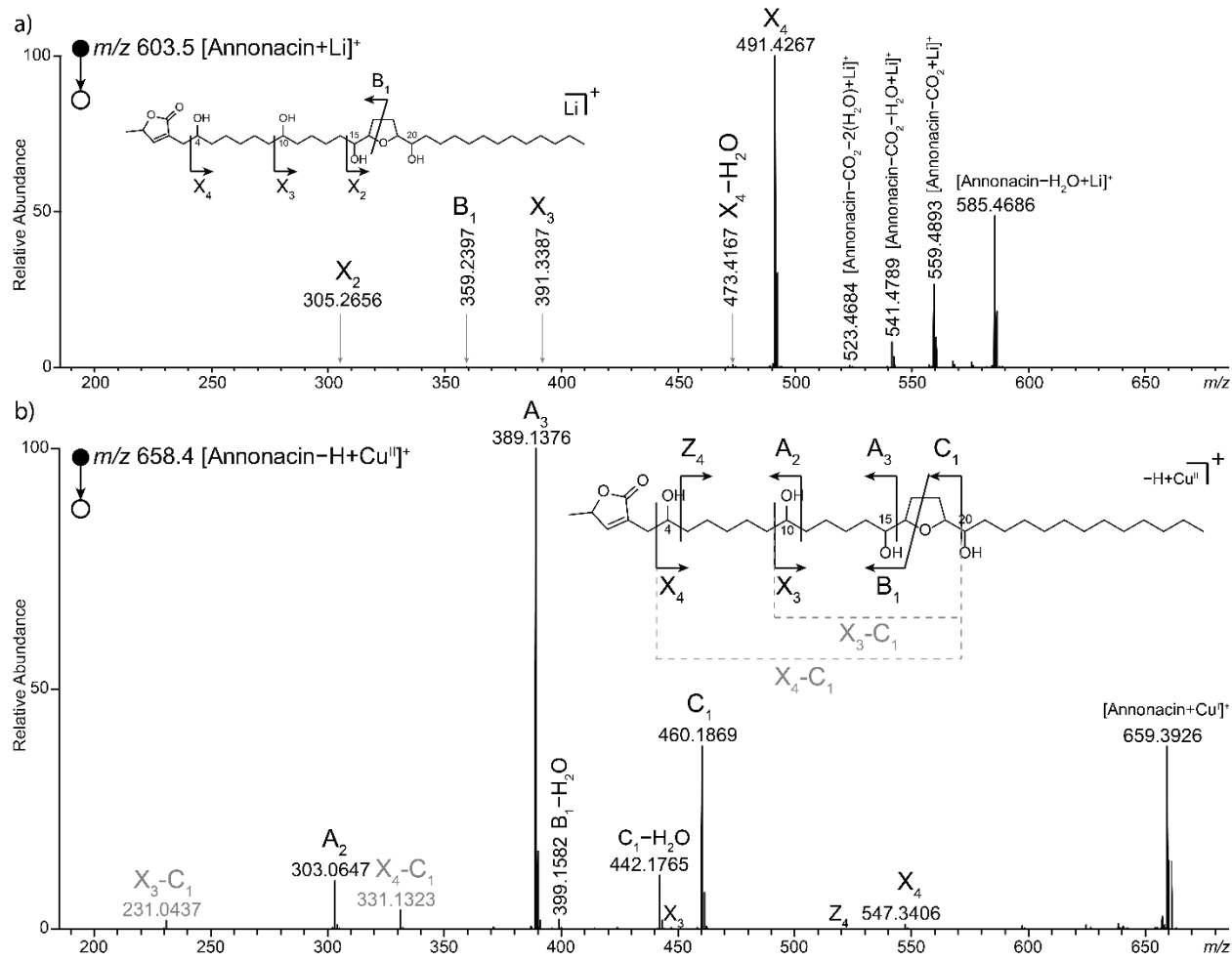
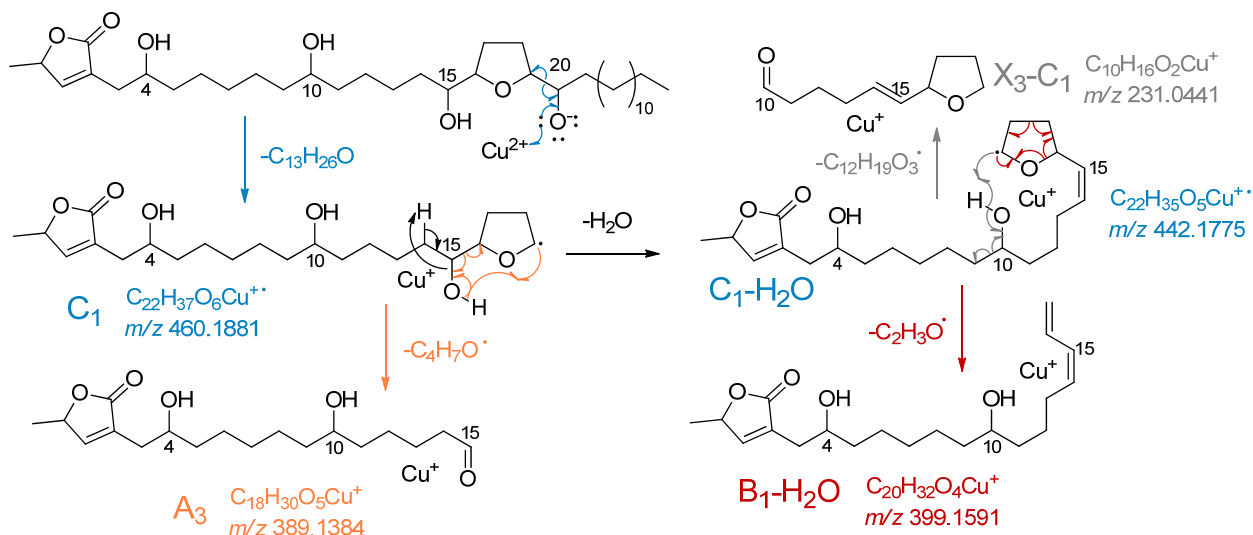


**Figure 1.** MS/MS spectra of a) [Annonacin+Li]<sup>+</sup> at 50 eV and b) [Annonacin–H+Cu<sup>II</sup>]<sup>+</sup> at 25 eV from ESI-LTQ-XL-Orbitrap instrument and the corresponding fragmentation schemes.

In order to better understand the MS/MS behavior of [acetogenins–H+Cu<sup>II</sup>]<sup>+</sup> ions, dissociation mechanisms were proposed. As previously shown on copper-containing ions dissociation, free radicals can be formed after copper reduction.<sup>11, 12</sup> This hypothesis was supported by formation of C<sub>1</sub> which is the only ion to show an odd-electron number. The proposed mechanism involves the stripping of an electron from the alkoxide on the C<sub>20</sub> atom followed by the formation of a neutral aldehyde containing the alkyl chain end, and a free radical on the THF function (Scheme 1). The formation of A and X even-electron ions resulted from the reduction of the copper. A similar

mechanism was proposed for the formation of these ions, depending on the electron delocalization side (Scheme S1); the copper removes an electron from the alkoxide function to form an aldehyde, followed by the displacement of an electron from the C-C bond on the lactone side to form the X ion, or on the THF side for the A ions, both losing a radical. The low intensity of X compared to A might be due to the location of copper cation on the electron-rich lactone, as acetogenins are probably folded around a central copper cation. Another explanation, confirmed by MS<sup>3</sup> experiments, is that A fragments can also be formed from C ions (Figure S3a). As C fragments retain a reduced copper, a second mechanism was proposed as a proton transfer on the radical THF followed by the formation of an aldehyde to give A. According to MS<sup>3</sup> experiments, B<sub>1</sub>-H<sub>2</sub>O ions are mainly formed from C<sub>1</sub> ions after a loss of H<sub>2</sub>O, probably from the C<sub>15</sub>, as A<sub>3</sub> is not observed from MS<sup>3</sup> experiments of C<sub>1</sub>-H<sub>2</sub>O (Figure S3b). The B<sub>1</sub>-H<sub>2</sub>O ions can be formed from the radical delocalization across the THF moiety (Scheme 1). Finally, we proposed a dissociation mechanism involving a proton transfer from the hydroxyl in C<sub>4</sub> or C<sub>10</sub> to the THF group to form X<sub>4</sub>-C<sub>1</sub> or X<sub>3</sub>-C<sub>1</sub> fragments respectively from C<sub>1</sub>-H<sub>2</sub>O.



**Scheme 1.** Proposed fragmentation pathways to form C<sub>1</sub> fragment (blue arrows) from [Annonacin-H+Cu<sup>II</sup>]<sup>+</sup>, A<sub>3</sub> (orange arrows) and C<sub>1</sub>-H<sub>2</sub>O (black arrows) from C<sub>1</sub> and B<sub>1</sub>-H<sub>2</sub>O (red arrows) and internal fragments (grey arrows) from C<sub>1</sub>-H<sub>2</sub>O (theoretical m/z values are displayed).

These mechanisms are consistent with MS<sup>n</sup> experiments carried out on annonacinone, differing from annonacin by the presence of a ketone instead of a hydroxyl function on the C<sub>10</sub>. Whereas C<sub>1</sub> and A<sub>3</sub> are major fragments, B<sub>1</sub>-H<sub>2</sub>O and X<sub>4</sub> ions were also observed as minor fragments, all

containing two hydrogens less than annonacin (Figure S4). By contrast, A<sub>2</sub>, X<sub>3</sub> and X<sub>3</sub>-C<sub>1</sub> ions were not observed as they involve either an alkoxide or a hydroxyl function on C<sub>10</sub>, replaced by a ketone in the case of annonacinone. Unfortunately, unlike what is observed on MS/MS spectra of the lithium adduct of annonacinone, no additional fragment ions allowed us determining the ketone position.

As lithium experiments did not succeed in determining hydroxyl positions in presence of bis-THF functions, squamocin, rolliniastatin-1 and diepomuricanin were investigated by MS/MS experiments from copper-adducted species [acetogenin-H+Cu<sup>II</sup>]<sup>+</sup>.<sup>8</sup> Figure 2 shows the MS/MS spectrum of the [Rolliniastatin-1-H+Cu<sup>II</sup>]<sup>+</sup> on different instruments.

A<sub>2</sub> and C<sub>2</sub> ions, corresponding to the C-C  $\alpha$ -cleavage of the bis-THF function and containing the lactone side, were observed as major fragments. In addition, the C<sub>1</sub> fragment ion corresponding to the C-C bond cleavage between the two THF, and the B<sub>1</sub> ion resulting from a ring opening process, were observed at a low intensity. These four fragments were also detected for diepomuricanin and squamocin, allowing an unambiguous structural characterization of bis-THF functions on acetogenins. Unfortunately, the hydroxyl function on the C<sub>4</sub> position cannot be located from ESI-LTQ-Orbitrap MS/MS experiments, as no X<sub>3</sub> or Z<sub>3</sub> ions were detected, whatever the collision energy parameters. However, from ESI-Q-TOF experiments, these ions were observed at *m/z* 573.3554 and *m/z* 544.3525, respectively (Figure 2c). The Z<sub>2</sub> ion (*m/z* 374.1746) was detected when performing MS/MS experiments on a Q-TOF instrument. The proposed mechanism for this odd-electron ion is similar to the one proposed to form C ions. It involves the initial deprotonation of the hydroxyl function on the C<sub>15</sub> and the stripping of an electron on this latter function by the copper, followed by the transfer of the electrons of the C-C bond between C<sub>15</sub> and C<sub>16</sub> to form the copper-free fragment A and the radical ion Z<sub>2</sub> (Scheme S2). This ion is only observed for analogues containing bis-THF function due to a favorable oxygen-rich environment for copper attachment.

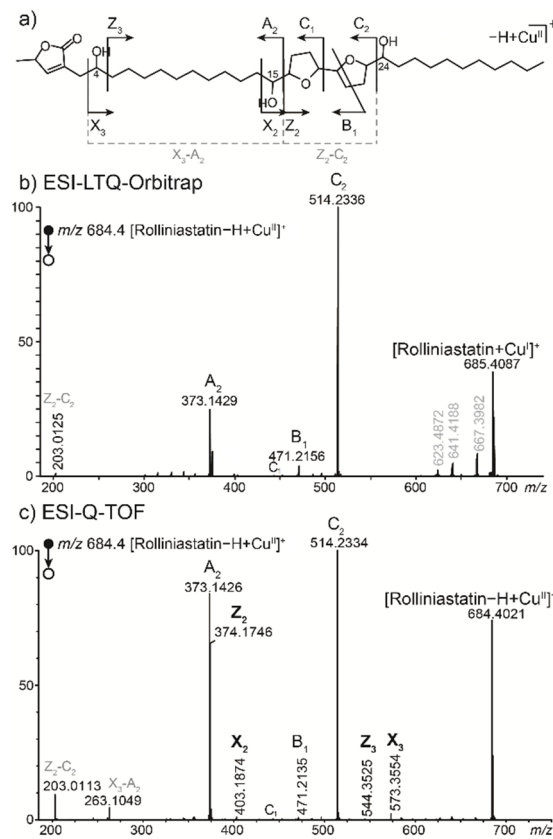
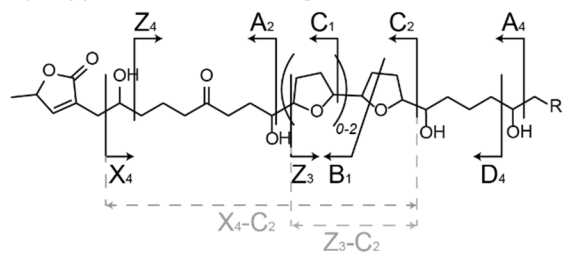


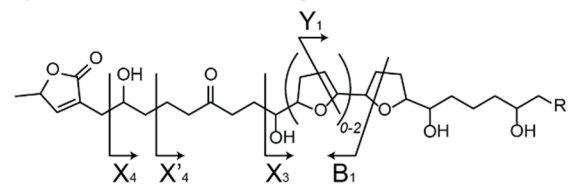
**Figure 2.** a) Dissociation scheme and MS/MS spectra of [Rolliniastatin-1-H+Cu<sup>II</sup>]<sup>+</sup> from b) ESI-LTQ-Orbitrap or c) ESI-Q-TOF instruments. Fragment ions annotated in bold were only observed during ESI-Q-TOF experiments.

MS/MS analysis of [acetogenins-H+Cu<sup>II</sup>]<sup>+</sup> allows the unambiguous characterization of hydroxyl and (bis-)THF functions from intense fragment ions. As an advantage to lithium-adduct species, structural-containing fragments for (bis-)THF functions are the most intense signals, which could be useful for molecular network approaches.<sup>18</sup> Nevertheless, unlike lithium adducts, MS/MS experiments of copper ions did not allow the ketone functions to be located as summarized on Scheme 2.

#### a) copper-adducted acetogenins



#### b) lithium-adducted acetogenins



Scheme 2. General CID fragmentation features observed for a) copper-cationized and b) lithium-cationized acetogenins.

MS<sup>n</sup> experiments performed on copper-adducted standards allowed us to propose a fragmentation pathway of acetogenins through ion filiation. Since more structurally informative fragments were observed in MS/MS (using a Q-TOF) than in MS<sup>2</sup> (using an Orbitrap), *Annona muricata* extracts were further analyzed on a Q-TOF mass analyzer. Infusion in post-LC column of copper salt to form [acetogenin-H+Cu<sup>II</sup>]<sup>+</sup> allowed us to localize the hydroxyl and THF functions, while a lithium salt was infused to localize ketone functions from [acetogenin+Li]<sup>+</sup> ions.

#### ***Acetogenins characterization from A. muricata extract by LC-MS/MS***

Acetogenin-rich *Annona muricata* seeds extract was analyzed by LC-MS/MS for dereplication purpose. The salt was introduced post-column, at 1 µM for CuSO<sub>4</sub> or at 10 µM for LiI in methanol. Sodiated species predominate in MS when introducing the copper salt since higher copper salt concentrations cause severe signal suppression. The MS profiles were comparable for [acetogenins-H+Cu<sup>II</sup>]<sup>+</sup> and [acetogenins+Li]<sup>+</sup> ions even if relative intensities were different for some analogues (Figure S6). Moreover, a better sensitivity was achieved with lithium as the affinity of acetogenins for alkali cations is higher than for Cu<sup>2+</sup>. IMS separation was performed in order to distinguish possible isomers and isobars not separated by LC (Figure S7). In fact, isobaric ions selected in the quadrupole can be differentiated by IMS even if baseline resolution is not achieved, which allows to clean MS/MS spectra as exemplified by the distinction of the <sup>65</sup>Cu isotope of [C<sub>37</sub>H<sub>65</sub>O<sub>7</sub>+<sup>65</sup>Cu]<sup>+</sup> ions at theoretical *m/z* 686.4003 and the <sup>63</sup>Cu signal of [C<sub>37</sub>H<sub>67</sub>O<sub>7</sub>+<sup>63</sup>Cu]<sup>+</sup> ions at *m/z* 686.4177 (Figure S8).

From targeted LC-IMS-MS/MS experiments, isomers were discriminated, and the large majority showed high quality MS/MS spectra, *i.e.* spectra with intense and specific fragment ions, allowing the identification of acetogenin analogues. [C<sub>35</sub>H<sub>59</sub>O<sub>7</sub>+Cu]<sup>+</sup>, [C<sub>35</sub>H<sub>61</sub>O<sub>7</sub>+Cu]<sup>+</sup>, [C<sub>35</sub>H<sub>63</sub>O<sub>7</sub>+Cu]<sup>+</sup>, [C<sub>35</sub>H<sub>61</sub>O<sub>8</sub>+Cu]<sup>+</sup>, [C<sub>35</sub>H<sub>63</sub>O<sub>8</sub>+Cu]<sup>+</sup>, [C<sub>37</sub>H<sub>65</sub>O<sub>7</sub>+Cu]<sup>+</sup>, [C<sub>37</sub>H<sub>67</sub>O<sub>7</sub>+Cu]<sup>+</sup> and [C<sub>37</sub>H<sub>65</sub>O<sub>8</sub>+Cu]<sup>+</sup> ions were fragmented at 20 eV collision energy, while the corresponding Li ions were activated at 65 eV in the transfer cell of the mass spectrometer. Seventy-seven common analogues were detected from the eight selected ion species using copper, and lithium in post column infusion. Most species were structurally characterized from copper adducts using the previously-established

dissociation rules. In total, 45 analogues could be fully identified except for the stereochemistry. 33 species could be fully characterized from copper adducts, and 12 species partially annotated from copper-adducted MS/MS spectra were identified by combining these results with the localization of the ketone function from MS/MS fragmentation of the lithiated species. Compared to lithium-adduct experiments previously published from the same *Annona muricata* extract, 21 new analogues were tentatively annotated according to specific fragmentation of Cu<sup>2+</sup>-cationized species.<sup>8</sup> It is important to note that the occurrence of diastereoisomers results in the presence of several chromatographic peaks for the same compound. Unfortunately, MS/MS does not allow for the determination of stereochemistry, therefore multiple species are annotated to the same compound in Table 1 such as Longimicin-B at t<sub>R</sub> 9.8 and 10.2 min, which refers to Longimicin-B-like compound.

**Table 1.** Identified analogues from targeted LC-MS/MS experiments of [acetogenins-H+Cu<sup>II</sup>]<sup>+</sup> and [acetogenins+Li]<sup>+</sup>.

Formula	t <sub>R</sub> (min)	Oxygen cycle	OH	CO	DB	Name
C <sub>35</sub> H <sub>60</sub> O <sub>7</sub>	5.3	16-19	4, 15, 20	10	[21-33]	M1
	10.2	8-11,12-15,16-19	4, 20			Gonionin
	12.2	4-8, 16-19	15, 20	10		Montanacin-D <sup>a</sup>
C <sub>35</sub> H <sub>62</sub> O <sub>7</sub>	4.3, 6.5, 7.0	16-19	4,10,15,20		[21-33]	Muricin G <sup>b</sup>
	6.0	16-19	12,15,20,34		[3-11]	
	7.4,8.0,8.2,8.6	16-19	4, 15, 20	10		Annonacinone <sup>a</sup>
	9.8, 10.2	12-15, 16-19	4, 11, 20			Longimicin-B
	11.7	10-13, 16-19	4, 15, 20			
	6.0	16-19	10,15,20,34			M2
C <sub>35</sub> H <sub>64</sub> O <sub>7</sub>	6.5, 7.0	16-19	4,10,15,20			Annonacin <sup>a</sup>
	7.5	16-19	4,8,15,20			Xylopiandin <sup>a</sup>
	8.0	16-19	4,12,15,20			Glacin-B
	8.3, 8.8	10-13	4,14,17,18			Gigantetrocin-A
	9.0, 9.4, 11.2	14-17	4,10,13,18			Goniothalamicin <sup>a</sup>
	3.2, 3.9	16-19	4,12,15,20	10		
C <sub>35</sub> H <sub>62</sub> O <sub>8</sub>	6.0	16-19	4,15,20,34	10		Goniodoninone
	2.2, 2.5	16-19	4,10,14,15,20			
	2.8	16-19	4,10,13,15,20			
	3.2, 3.5, 4.4	16-19	4,10,11,15,20			Annomuricin-B
	4.9	16-19	4,10,15,20,34			Goniodonin <sup>a</sup>
	7.9	16-19	4,10,15,20		[21-35]	Xylomatenin <sup>b</sup>
C <sub>37</sub> H <sub>66</sub> O <sub>7</sub>	9.5	16-19, 20-23	4, 15, 24			Rolliniastatin
	10.3	18-21	4, 17, 22	12		Annomontacin-12-one
	11.1, 11.4	10-13	4,14,17,18		[19-35]	Gigantetronenin <sup>c</sup>
	12.1, 12.6	18-21	4, 17, 22	10		Annomontacin-10-one
	12.2, 13.0	14-17, 18-21	10, 13, 22			Longimicin-D
	13.4, 13.6	14-17, 18-21	[4-12],13,22			
	14.4	10-13, 18-21	14, 17, 22			4-Deoxygigantecin
	10.4,11.0,11.3	18-21	4,10,17,22			Annomontacin

$C_{37}H_{68}O_7$	12.1, 12.6	16-19	4,10,15,20	Xylomaticin
	2.5	16-20	4,10,14,15,20	
$C_{37}H_{66}O_8$	5.3, 5.6	14-17, 18-21	4,10,13,22	Hydroxyglaucanetin
	6.4	10-13, 18-21	4,14,17,22	Gigantecin

<sup>a</sup> compounds identified from LC-MS/MS experiments with lithium in a previous study on the same sample of *Annona muricata*.<sup>8</sup> Compounds named from the literature with assumptions of the double bound (DB) localization between <sup>b</sup> C<sub>23</sub>-C<sub>24</sub> or <sup>c</sup> C<sub>21</sub>-C<sub>22</sub>.

A total of 45 acetogenin analogues were characterized using the complementary information deduced from MS/MS spectra of [acetogenins-H+Cu<sup>II</sup>]<sup>+</sup> and [acetogenins+Li]<sup>+</sup>. Finally, 8 compounds were partially annotated since neither lithium adducts nor copper adducts allow the localization of double bonds. Among these eight compounds, six can be attributed based on known compounds in the literature such as muricin G, xylomatenin and gigantetronenin with double bound localizations on C<sub>23</sub>-C<sub>24</sub>, C<sub>23</sub>-C<sub>24</sub> and C<sub>21</sub>-C<sub>22</sub>, respectively.

From the newly observed analogues in *Annona muricata* a larger diversity in acetogenins backbones was enlightened compared to previous study, thanks to copper adduction.<sup>8</sup> Indeed, the gonionin analogue observed at 10.2 min exhibits 3 stacked THF rings and was unambiguously characterized from copper adduct analysis, while lithium adduct experiments could lead to misinterpretation. In addition, LC-MS/MS analysis with lithium cationization did not succeed to highlight double THF functions, whereas many analogues containing stacked THF ring (10-hydroxyglaucanetin, rolliniastatin, longimicin -B and -D) or separated THF rings (4-deoxygigantecin, gigantecin) are annotated with copper. Moreover, we assume that the copper ion is most probably chelated by adjacent THF rings which are electron-rich sites, allowing the characterization of analogues with THF functions away from the lactone such as annomontacin and annomontacinone-like compounds which could not be structurally distinguished from LC-MS/MS analysis with lithium. Indeed, lithium experiments yield mainly X<sub>n</sub> fragments, the intensity of which decreases when the distance between the lactone and the THF function increases.

In order to highlight the structural variations at the level of the acetogenin backbone, we generated molecular networks (MN) from lithium- and copper-cationized species using MetGem<sup>14</sup> software. As previously mentioned, lithium adducts of acetogenins yield mainly losses of H<sub>2</sub>O, CO<sub>2</sub> and of the lactone part (Figure 1a), resulting in cosine scores around 0.9 between analogues (Figure S20). The corresponding molecular network was then built after the removal of non-specific fragment ions (losses of H<sub>2</sub>O and CO<sub>2</sub> and combination) to increase the specificity (Figure S21). Even after

the removal of non-specific losses (corresponding to a filtering of peaks at  $\pm$  100 Da from the precursor ion in MetGem), cosine scores are higher than 0.8 due to the lactone related ion at  $m/z$  112.05 and consecutive losses of H<sub>2</sub>O representing about 0.7 in cosine score of each node pairs in the main cluster. The score of low intensity fragments which allow the location of hydroxyl, ketone or THF groups is then negligible. For example, annonacin-like compounds share a cosine score of 0.97 with the xylomaticin, an analogue only differing in the terminal carbon chain length. The annonacin/annonacinone-like pair also exhibits a mean cosine score of 0.93. Consequently, the differentiations in terms of acetogenin backbone are very poor from the MN constructed from the MS/MS data of lithium-cationized species. Moreover, the annonacin/gigantreonenin and annonacinone/gonionin pairs also show a cosine score higher than 0.9 while both THF and hydroxyl positions are different. Finally, ions with hydroxylated lactone or a ring next to the lactone such as montanacin-D-like compounds are observed into different ion clusters.

By contrast, MN built on MS/MS data from copper-cationized species shows a higher cosine scores heterogeneity thanks to specific and intense fragment ions (Figure S20). The resulting MN introduced in Figure 3 allows distinction between THF ring localization. Therefore, THF ring between C<sub>16</sub> and C<sub>19</sub> (annotated A) represents the major part of the main cluster as they are the most abundant in *Annona muricata*.<sup>17</sup> In this cluster A, we could also distinguish analogues substituted on C<sub>10</sub> (light blue Figure 3) or on C<sub>12</sub> (dark blue Figure 3) by either a ketone or a hydroxyl moiety. THF rings between C<sub>14</sub> and C<sub>17</sub> (annotated B) represent a minor part of this cluster, like analogues with THF rings between C<sub>18</sub> and C<sub>21</sub> (annotated C), and they can both be distinguished from other THF ring locations.

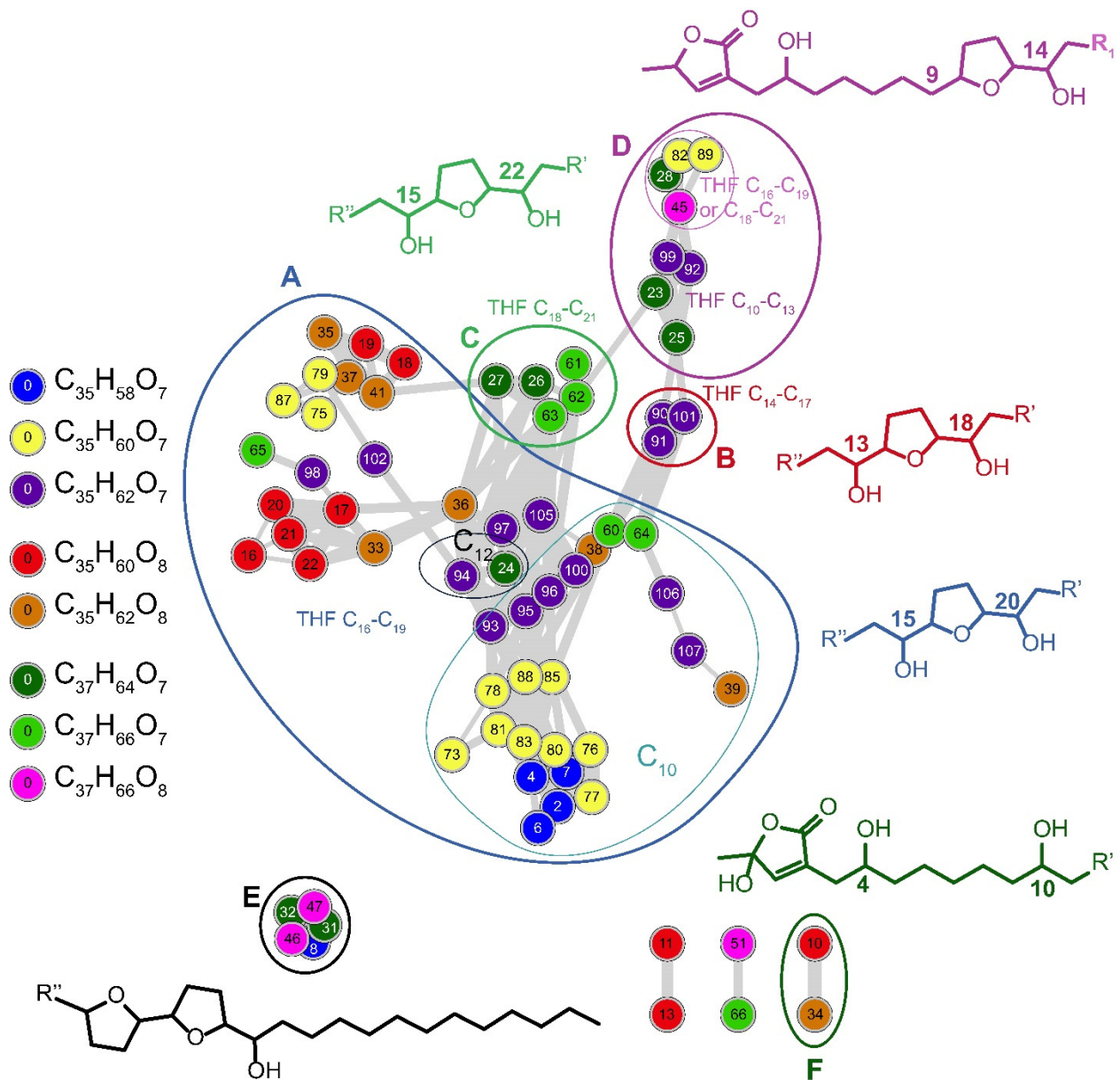


**Figure 3.** Molecular network of 8 copper-adducted precursor ions from an *Annona muricata* extract. Nodes colors are based on the *m/z* of the precursor ion as followed: 654.35 in blue, 656.36 in yellow, 658.38 in purple, 672.37 in red, 674.38 in orange, 684.40 in dark green, 686.42 in pale green and 700.40 in pink.

Finally, analogues having mono-hydroxylated THF ring between C<sub>10</sub> and C<sub>13</sub> (annotated D) are localized in the last part of this cluster, including additional doubly-hydroxylated THF rings as the signal intensities of mono-hydroxylated compounds showed higher intensities. Clusters B, C and D could be fully characterized. The cluster annotated E corresponds to bis-adjacent-hydroxylated THF rings and a C<sub>13</sub> chain length, while the cluster F composed of two nodes corresponds to hydroxylated lactones with different chain lengths. The MN built on MS/MS data from copper-

cationized species is therefore more structurally informative than the one related to lithium-cationized species, mainly showing distinctions related to substitutions adjacent to the lactone only.

## Conclusions

Collision induced dissociation of  $[M-H+Cu^{II}]^+$  ions from Annonaceous acetogenins provides a simple and robust approach to obtain highly informative MS/MS spectra. Compared to CID of  $[M+Li]^+$  ions, copper-cationized acetogenins lead to intense fragment ions resulting from the cleavage of C-C bonds on both sides of the THF rings. In addition, C-C bond cleavages in alpha of the hydroxyl groups allows the localization of hydroxyl functions along the acetogenins skeleton. These specific fragment ions mainly involved radical dissociation mechanisms that occur in presence of the copper cation. Using CuSO<sub>4</sub> salt in post-column infusion allowed us to identify 45 analogues in LC-MS/MS from an *Annona muricata* extract, which is twice more than using a lithium salt solution.

This MS/MS method together with molecular network data classification now paves the way to a high throughput approach of the acetogenins dereplication in complex extracts. Moreover, copper-cationized species is confirmed to be of high interest for the structural characterization of oxygen-rich molecules by MS/MS. This approach should be extended to other polyketides, such as complex polyols.

## Acknowledgments

The authors thank the ANR CHARMMMAT (ANR11-LABX-0039) for the post-doctoral fellowship to S.P. and the Ile-de-France DIM Analytics for MOBICS project. L.L. is indebted to the CNRS-ICSN and to the “*Fondation pour le développement de la chimie des substances naturelles et ses applications*” for a Ph.D. research fellowship. S.P. would also like to warmly acknowledge Isabelle Schmitz-Afonso for her help in data treatment to generate the molecular networks.

## References

- (1) Bermejo, A.; Figadere, B.; Zafra-Polo, M. C.; Barrachina, I.; Estornell, E.; Cortes, D. Acetogenins from Annonaceae: recent progress in isolation, synthesis and mechanisms of action. *Nat. Prod. Rep.* **2005**, *22* (2), 269-303.
- (2) Neske, A.; Ruiz Hidalgo, J.; Cabedo, N.; Cortes, D. Acetogenins from Annonaceae family. Their potential biological applications. *Phytochem.* **2020**, *174*, 112332. Bonneau, N.; Cynober, T.; Jullian, J. C.; Champy, P. (1) H qNMR Quantification of Annonaceous Acetogenins in Crude Extracts of *Annona muricata* L. Fruit Pulp. *Phytochem. Anal.* **2017**, *28* (4), 251-256.
- (3) Caparros-Lefebvre, D.; Elbaz, A. Possible relation of atypical parkinsonism in the French West Indies with consumption of tropical plants: a case-control study. *Lancet* **1999**, *354* (9175), 281-286. Hernández-Fuentes, G. A.; García-Argáez, A. N.; Peraza Campos, A. L.; Delgado-Enciso, I.; Muñiz-Valencia, R.; Martínez-Martínez, F. J.; Toninello, A.; Gómez-Sandoval, Z.; Mojica-Sánchez, J. P.; Dalla Via, L.; et al. Cytotoxic Acetogenins from the Roots of *Annona purpurea*. *Int. J. Mol. Sci.* **2019**, *20* (8), 1870. Agu, K. C.; Okolie, N. P.; Falodun, A.; Engel-Lutz, N. In vitro anticancer assessments of *Annona muricata* fractions and in vitro antioxidant profile of fractions and isolated acetogenin (15-acetyl guanaccone). *J. Cancer Res. Pract.* **2018**, *5* (2), 53-66.
- (4) Jacobo-Herrera, N.; Pérez-Plasencia, C.; Castro-Torres, V. A.; Martínez-Vázquez, M.; González-Esquínca, A. R.; Zentella-Dehesa, A. Selective Acetogenins and Their Potential as Anticancer Agents. *Front. Pharmacol.* **2019**, *10* (783).
- (5) Allegrand, J.; Touboul, D.; Schmitz-Afonso, I.; Guérineau, V.; Giuliani, A.; Le Ven, J.; Champy, P.; Laprévote, O. Structural study of acetogenins by tandem mass spectrometry under high and low collision energy. *Rapid Commun. Mass Spectrom.* **2010**, *24* (24), 3602-3608.
- (6) Meneses da Silva, E. L.; Roblot, F.; Hocquemiller, R.; Serani, L.; Laprévote, O. Structure elucidation of annoheptocins, two new heptahydroxylated C37 acetogenins by high-energy collision-induced dissociation tandem mass spectrometry. *Rapid Commun. Mass Spectrom.* **1998**, *12* (23), 1936-1944.
- (7) Laprévote, O.; C. Das, B. Structural Elucidation of Acetogenins from Annonaceae by Fast Atom Bombardment Mass Spectrometry. *Tetrahedron* **1994**, *50* (28), 8479-8490.
- (8) Le Ven, J.; Schmitz-Afonso, I.; Lewin, G.; Laprévote, O.; Brunelle, A.; Touboul, D.; Champy, P. Comprehensive characterization of Annonaceous acetogenins within a complex extract by HPLC-ESI-LTQ-Orbitrap® using post-column lithium infusion. *J. Mass Spectrom.* **2012**, *47* (11), 1500-1509.
- (9) Bonneau, N.; Baloul, L.; Bajin ba Ndob, I.; Sénejoux, F.; Champy, P. The fruit of *Annona squamosa* L. as a source of environmental neurotoxins: From quantification of squamocin to annotation of Annonaceous acetogenins by LC-MS/MS analysis. *Food Chem.* **2017**, *226*, 32-40.
- (10) Laboureur, L.; Bonneau, N.; Champy, P.; Brunelle, A.; Touboul, D. Structural Characterisation of Acetogenins from *Annona muricata* by Supercritical Fluid Chromatography Coupled to High-Resolution Tandem Mass Spectrometry. *Phytochem. Anal.* **2017**, *28* (6), 512-520.
- (11) Afonso, C.; Riu, A.; Xu, Y.; Fournier, F.; Tabet, J.-C. Structural characterization of fatty acids cationized with copper by electrospray ionization mass spectrometry under low-energy collision-induced dissociation. *J. Mass Spectrom.* **2005**, *40* (3), 342-349.
- (12) Lopes, N. P.; Stark, C. B. W.; Staunton, J.; Gates, P. J. Evidence for gas-phase redox chemistry inducing novel fragmentation in a complex natural product. *Org. Biomol. Chem.* **2004**, *2* (3), 358-363.

- (13) Tureček, F. Copper-biomolecule complexes in the gas phase. The ternary way. *Mass Spectrom. Rev.* **2007**, *26* (4), 563-582. Campos, P.-E.; Herbette, G.; Chendo, C.; Clerc, P.; Tintillier, F.; de Voogd, N. J.; Papanagnou, E.-D.; Trougakos, I. P.; Jerabek, M.; Bignon, J.; et al. Osirisynes G-I, New Long-Chain Highly Oxygenated Polyacetylenes from the Mayotte Marine Sponge Haliclona sp. *Mar. Drugs* **2020**, *18* (7), 350. Felder, T.; Röhrich, A.; Stephan, H.; Schalley, C. A. Fragmentation reactions of singly and doubly protonated thiourea- and sugar-substituted cyclams and their transition-metal complexes. *J. Mass Spectrom.* **2008**, *43* (5), 651-663. Gatlin, C. L.; Turecek, F.; Vaisar, T. Copper(II) amino acid complexes in the gas phase. *J. Amer. Chem. Soc.* **1995**, *117* (12), 3637-3638. Crevelin, E. J.; Possato, B.; Lopes, J. L. C.; Lopes, N. P.; Crotti, A. E. M. Precursor Ion Scan Mode-Based Strategy for Fast Screening of Polyether Ionophores by Copper-Induced Gas-Phase Radical Fragmentation Reactions. *Anal. Chem.* **2017**, *89* (7), 3929-3936.
- (14) Olivon, F.; Elie, N.; Grelier, G.; Roussi, F.; Litaudon, M.; Touboul, D. MetGem Software for the Generation of Molecular Networks Based on the t-SNE Algorithm. *Anal. Chem.* **2018**, *90* (23), 13900-13908.
- (15) Pluskal, T.; Castillo, S.; Villar-Briones, A.; Oresic, M. MZmine 2: modular framework for processing, visualizing, and analyzing mass spectrometry-based molecular profile data. *BMC Bioinformatics* **2010**, *11*, 395. Olivon, F.; Grelier, G.; Roussi, F.; Litaudon, M.; Touboul, D. MZmine 2 Data-Preprocessing To Enhance Molecular Networking Reliability. *Anal. Chem.* **2017**, *89* (15), 7836-7840.
- (16) McCloud, T. G.; Smith, D. L.; Chang, C. J.; Cassady, J. M. Annonacin, a novel, biologically active polyketide from *Annona densicoma*. *Experientia* **1987**, *43* (8), 947-949.
- (17) Liaw, C. C.; Liou, J. R.; Wu, T. Y.; Chang, F. R.; Wu, Y. C. Acetogenins from Annonaceae. *Prog. Chem. Org. Nat. Prod.* **2016**, *101*, 113-230.
- (18) Scheubert, K.; Hufsky, F.; Petras, D.; Wang, M.; Nothias, L.-F.; Dührkop, K.; Bandeira, N.; Dorrestein, P. C.; Böcker, S. Significance estimation for large scale metabolomics annotations by spectral matching. *Nat. Commun.* **2017**, *8* (1), 1494.

# **Dereplication of acetogenins from *Annona muricata* by combining tandem mass spectrometry after lithium and copper post-column cationization and molecular networks**

Salomé Poyer,<sup>1\*</sup> Laurent Laboureur,<sup>1</sup> Téo Hebra,<sup>1</sup> Nicolas Elie,<sup>1</sup> Guillaume Van der Rest,<sup>2</sup> Jean-Yves Salpin,<sup>3,4</sup> Pierre Champy,<sup>5</sup> David Touboul<sup>1\*</sup>

1. Université Paris-Saclay, CNRS, Institut de Chimie des Substances Naturelles, UPR 2301, 91198, Gif-sur-Yvette, France.
2. Université Paris-Saclay, CNRS, Institut de Chimie Physique, 91405, Orsay, France.
3. Université Paris-Saclay, Univ Evry, CNRS, LAMBE, 91025, Evry-Courcouronnes, France.
4. LAMBE, CY Cergy Paris Université, CNRS, 95000 Cergy, France.
5. Université Paris-Saclay, CNRS, BioCIS, 92290, Châtenay-Malabry, France.

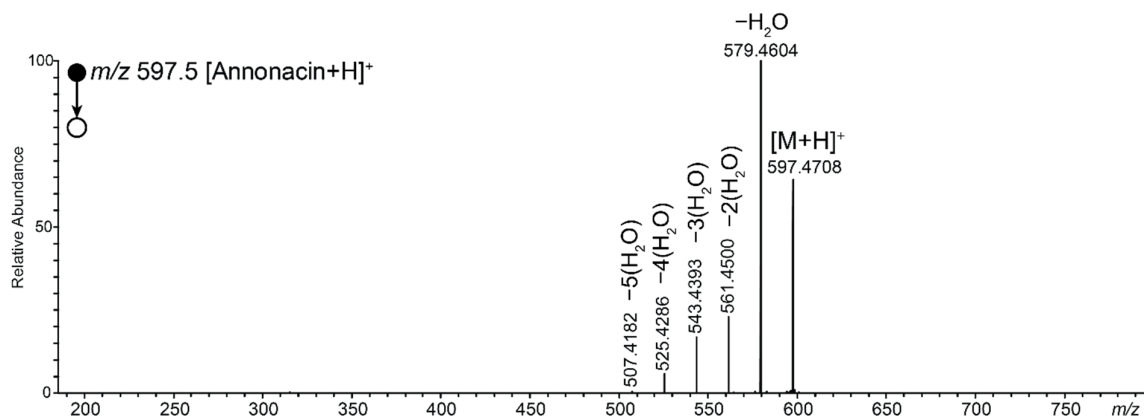
## **Supporting Information**

Figure S1. MS/MS spectrum of [Annonacin+H] <sup>+</sup> at 20 eV from ESI-LTQ-Orbitrap instrument	4
Figure S2. MS spectrum of annonacin standard solution at 10 mg/L in a methanolic solution at 100 μM of CuSO <sub>4</sub> from ESI-LTQ-Orbitrap instrument.....	4
Figure S3. MS <sup>3</sup> spectra from [Annonacin-H+Cu <sup>II</sup> ] <sup>+</sup> of a) C <sub>1</sub> at <i>m/z</i> 460.2 and b) C <sub>1</sub> -H <sub>2</sub> O at <i>m/z</i> 442.2 at 15 eV from ESI-LTQ-Orbitrap instrument.....	5
Table S1. Exact mass measurement from MS/MS spectrum of [Annonacin-H+Cu <sup>II</sup> ] <sup>+</sup> showed in Figure 1.....	5
Figure S4. MS/MS spectrum of [Annonacinone-H+Cu <sup>II</sup> ] <sup>+</sup> at 50 eV from ESI-LTQ-Orbitrap device and the corresponding fragmentation scheme.....	6
Table S2. Exact mass measurement from MS/MS spectrum of [Annonacinone-H+Cu <sup>II</sup> ] <sup>+</sup> showed in Figure S4. ....	6
Table S3. Exact mass measurement from MS/MS spectrum of [Rolliniastatin-1-H+Cu <sup>II</sup> ] <sup>+</sup> from Q-TOF experiments showed in Figure 2c. ....	7
Scheme S1. Proposed dissociation mechanism for Z <sub>2</sub> (purple arrows) fragment ion from [Rolliniastatin-H+Cu <sup>II</sup> ] <sup>+</sup> .....	7
Figure S5. MS/MS spectra and the corresponding fragmentation scheme of a) [Squamocin-H+Cu <sup>II</sup> ] <sup>+</sup> at 35 eV and b) [Desacetyl-uvaricin-H+Cu <sup>II</sup> ] <sup>+</sup> at 10 eV from ESI-Q-TOF instrument.....	8
Figure S6. Extracted ion chromatogram of LC-MS spectra using in post-column infusion a) MeOH, b) MeOH with LiI at 10 μM and c) MeOH with CuSO <sub>4</sub> at 1 μM.....	9
Figure S7. MS/MS spectra from LC-IMS-MS/MS experiments a) without using the IMS dimension, and after IMS differentiation of c) [2(annomontacinone+Cu) <sup>2+</sup> ( <i>m/z</i> 654.4468) vs d) [Gonionin-H+Cu] <sup>+</sup> ( <i>m/z</i> 654.3551) from the b) extracted IMS spectrum of the corresponded tr. ....	10
Figure S8. a) Extracted ion mobility spectrum of tr 10.2 min from LC-IMS-MS/MS of <i>m/z</i> 686.4 and extracted MS/MS spectra of b) left part of the ion mobility peak corresponding to [C <sub>37</sub> H <sub>65</sub> O <sub>7</sub> + <sup>65</sup> Cu] <sup>+</sup> , which was not attributed and c) right part of the ion mobility peak corresponding to [Annomontacin-H+ <sup>63</sup> Cu] <sup>+</sup> .....	11
Figure S9. MS/MS spectra of [M1-H+Cu <sup>II</sup> ] <sup>+</sup> at 20 eV (top) and of [M1+Li] <sup>+</sup> at 65 eV (bottom) from LC-ESI-QTOF-MS/MS experiments and the corresponding fragmentation scheme.....	12

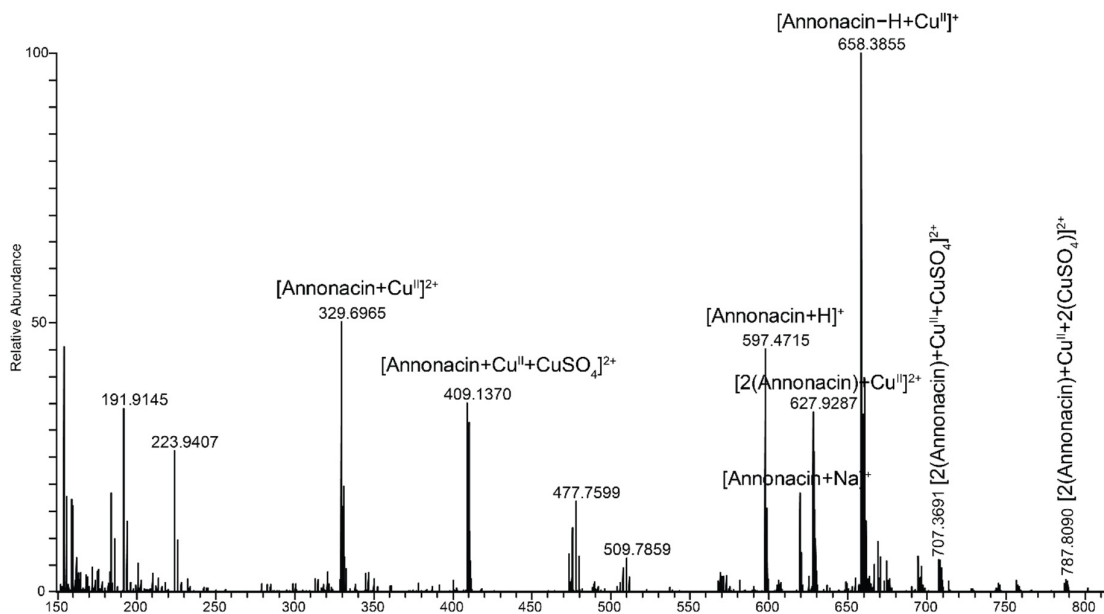
Figure S10. MS/MS spectra of [Goniodonin–H+Cu <sup>II</sup> ] <sup>+</sup> at 20 eV (top) and of [Goniodonin+Li] <sup>+</sup> at 65 eV (bottom) from LC-ESI-QTOF-MS/MS experiments and the corresponding fragmentation scheme.....	12
Figure S11. MS/MS spectra of [Montanacin-D–H+Cu <sup>II</sup> ] <sup>+</sup> at 20 eV (top) and of [Montanacin-D+Li] <sup>+</sup> at 65 eV (bottom) from LC-ESI-QTOF-MS/MS experiments and the corresponding fragmentation scheme.....	13
Figure S12. MS/MS spectra of [Muricin-G–H+Cu <sup>II</sup> ] <sup>+</sup> at 20 eV (top) and of [Muricin-G+Li] <sup>+</sup> at 65 eV (bottom) from LC-ESI-QTOF-MS/MS experiments and the corresponding fragmentation scheme.....	13
Figure S13. MS/MS spectra of [M2–H+Cu <sup>II</sup> ] <sup>+</sup> at 20 eV (top) and of [M2+Li] <sup>+</sup> at 65 eV (bottom) from LC-ESI-QTOF-MS/MS experiments and the corresponding fragmentation scheme.....	14
Figure S14. MS/MS spectra of [Annomontacin–H+Cu <sup>II</sup> ] <sup>+</sup> at 20 eV (top) and of [Annomontacin+Li] <sup>+</sup> at 65 eV (bottom) from LC-ESI-QTOF-MS/MS experiments and the corresponding fragmentation scheme.....	15
Figure S15. MS/MS spectra of [Xylomaticin–H+Cu <sup>II</sup> ] <sup>+</sup> at 20 eV (top) and of [Xylomaticin+Li] <sup>+</sup> at 65 eV (bottom) from LC-ESI-QTOF-MS/MS experiments and the corresponding fragmentation scheme.....	16
Figure S16. MS/MS spectra of [Xylomatenin–H+Cu <sup>II</sup> ] <sup>+</sup> at 20 eV (top) and of [Xylomatenin+Li] <sup>+</sup> at 65 eV (bottom) from LC-ESI-QTOF-MS/MS experiments and the corresponding fragmentation scheme.....	17
Figure S17. MS/MS spectra of [Rolliniastatin–H+Cu <sup>II</sup> ] <sup>+</sup> at 20 eV (top) and of [Rolliniastatin+Li] <sup>+</sup> at 65 eV (bottom) from LC-ESI-QTOF-MS/MS experiments and the corresponding fragmentation scheme.....	18
Figure S18. MS/MS spectra of [Longimicin-D–H+Cu <sup>II</sup> ] <sup>+</sup> at 20 eV (top) and of [Longimicin-D+Li] <sup>+</sup> at 65 eV (bottom) from LC-ESI-QTOF-MS/MS experiments and the corresponding fragmentation scheme.....	19
Figure S19. MS/MS spectra of [Annomontacin-10-one–H+Cu <sup>II</sup> ] <sup>+</sup> at 20 eV (top) and of [Annomontacin-10-one+Li] <sup>+</sup> at 65 eV (bottom) from LC-ESI-QTOF-MS/MS experiments and the corresponding fragmentation scheme.....	20
Table S4. Identified analogues from LC-MS/MS experiments of [acetogenins–H+Cu <sup>II</sup> ] <sup>+</sup> .....	21

Figure S20. Cosine score plots of a) Li molecular network (MN) with a 14 Da window limit in purple vs Li MN with 100 Da window limit in yellow and b) comparison between Li MN in yellow and Cu MN in purple ..... 22

Figure S21. Molecular network of 8 lithiated precursor ions from an *Annona muricata* extract. Nodes colors are based on the *m/z* of the precursor ion as followed: 599.45 in blue, 601.46 in yellow, 603.48 in purple, 617.46 in red, 619.47 in orange, 629.49 in dark green, 631.52 in pale green and 645.49 in pink. ..... 23



**Figure S1.** MS/MS spectrum of  $[\text{Annonacin}+\text{H}]^+$  at 20 eV from ESI-LTQ-Orbitrap instrument



**Figure S2.** MS spectrum of annonacin standard solution at 10 mg/L in a methanolic solution at 100  $\mu\text{M}$  of  $\text{CuSO}_4$  from ESI-LTQ-Orbitrap instrument.

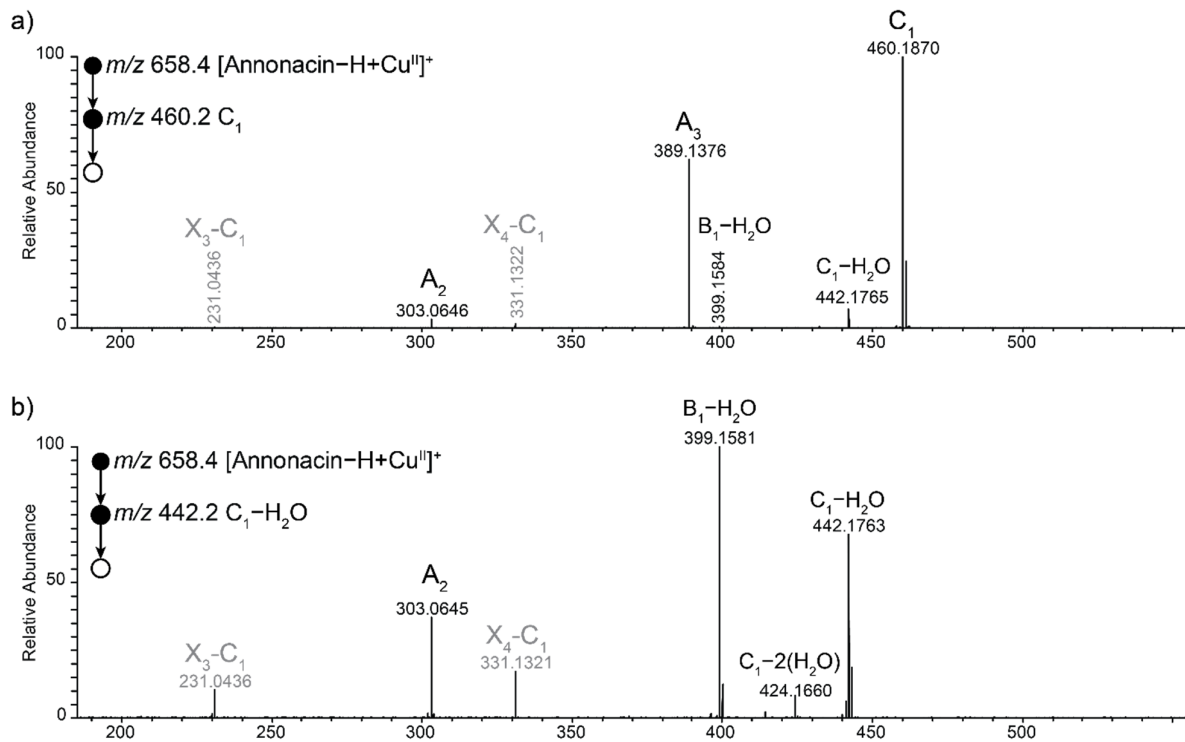


**Figure S3.**  $MS^3$  spectra from  $[Annonacin-H+Cu^{II}]^+$  of a)  $C_1$  at  $m/z$  460.2 and b)  $C_1-H_2O$  at  $m/z$  442.2 at 15 eV from ESI-LTQ-Orbitrap instrument.

**Table S1.** Exact mass measurement from MS/MS spectrum of  $[Annonacin-H+Cu^{II}]^+$  showed in Figure 1.

Ion	Experimental $m/z$	Theoretical $m/z$	$\Delta ppm$	Chemical formula
$[Annonacin-H+Cu^{II}]^+$	n.d.	658.3864	-	$C_{35}H_{63}O_7Cu^+$
$X_4$	547.3406	547.3418	-2.2	$C_{29}H_{56}O_5Cu^+$
$Y_4$	518.3367	518.3391	-4.6	$C_{28}H_{55}O_4Cu^{+•}$
$C_1$	460.1869	460.1881	-2.6	$C_{22}H_{37}O_6Cu^{+•}$
$X_3$	447.2520	447.2530	-2.2	$C_{23}H_{44}O_4Cu^+$
$C_1-H_2O$	442.1765	442.1775	-2.3	$C_{22}H_{35}O_5Cu^{+•}$
$C_1-2(H_2O)$	424.1661	424.1669	-1.9	$C_{22}H_{33}O_4Cu^{+•}$
$B_1-H_2O$	399.1582	399.1591	-2.3	$C_{20}H_{32}O_4Cu^+$
$A_3$	389.1376	389.1384	-2.1	$C_{18}H_{30}O_5Cu^+$
$X_4-C_1$	331.1323	331.1329	-1.8	$C_{16}H_{28}O_3Cu^+$
$A_2$	303.0647	303.0652	-1.6	$C_{13}H_{20}O_4Cu^+$
$X_3-C_1$	231.0437	231.0441	-1.7	$C_{10}H_{16}O_2Cu^+$

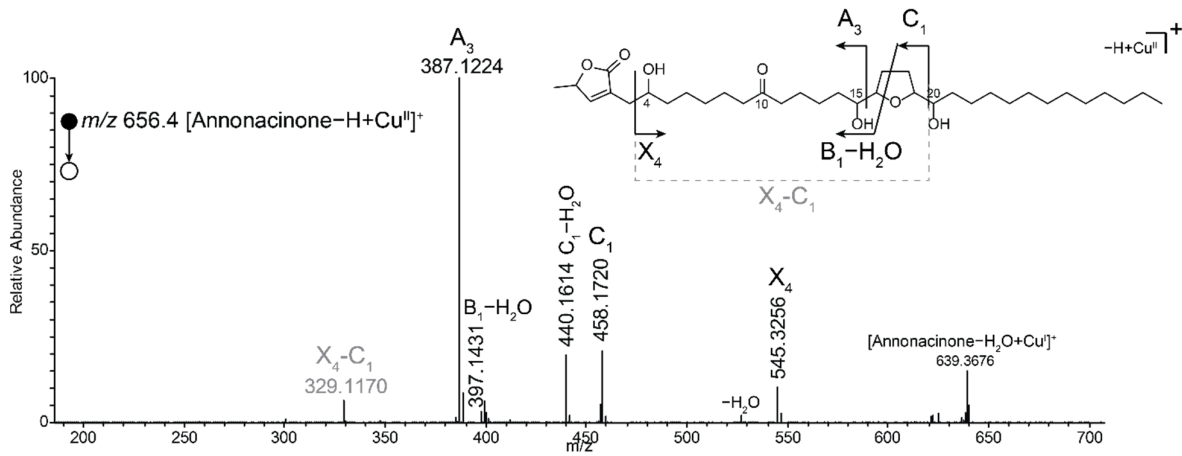


**Figure S4.** MS/MS spectrum of  $[\text{Annonacinone}-\text{H}+\text{Cu}^{\text{II}}]^+$  at 50 eV from ESI-LTQ-Orbitrap device and the corresponding fragmentation scheme.

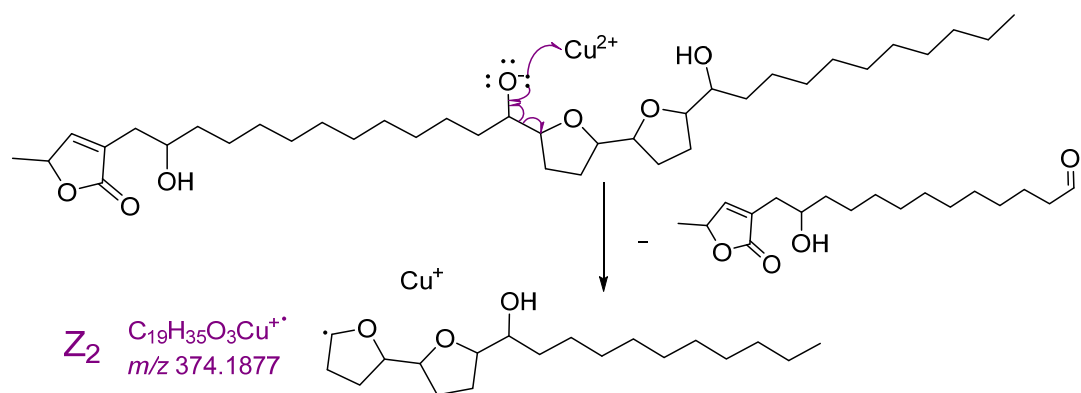
**Table S2.** Exact mass measurement from MS/MS spectrum of  $[\text{Annonacinone}-\text{H}+\text{Cu}^{\text{II}}]^+$  showed in Figure S4.

Ion	Experimental $m/z$	Theoretical $m/z$	$\Delta \text{ppm}$	Chemical formula
$[\text{Annonacinone}-\text{H}+\text{Cu}^{\text{II}}]^+$	n.d.	656.3708	-	$\text{C}_{35}\text{H}_{61}\text{O}_7\text{Cu}^+$
$[\text{Annonacinone}-\text{H}_2\text{O}+\text{Cu}^{\text{I}}]^+$	639.3676	639.3680	-0.6	$\text{C}_{35}\text{H}_{60}\text{O}_6\text{Cu}^+$
$\text{X}_4$	545.3256	545.3262	-1.1	$\text{C}_{29}\text{H}_{54}\text{O}_5\text{Cu}^+$
$\text{C}_1$	458.1720	458.1724	-0.9	$\text{C}_{22}\text{H}_{35}\text{O}_6\text{Cu}^{+\bullet}$
$\text{C}_1-\text{H}_2\text{O}$	440.1614	440.1619	-1.1	$\text{C}_{22}\text{H}_{33}\text{O}_5\text{Cu}^{+\bullet}$
$\text{B}_1-\text{H}_2\text{O}$	397.1431	397.1435	-1.0	$\text{C}_{20}\text{H}_{30}\text{O}_4\text{Cu}^+$
$\text{A}_3$	387.1224	387.1227	-0.8	$\text{C}_{18}\text{H}_{28}\text{O}_5\text{Cu}^+$
$\text{X}_4-\text{C}_1$	329.1170	329.1172	-0.6	$\text{C}_{16}\text{H}_{26}\text{O}_3\text{Cu}^+$

**Table S3.** Exact mass measurement from MS/MS spectrum of [Rolliniastatin-1-H+Cu<sup>II</sup>]<sup>+</sup> from Q-TOF experiments showed in Figure 2c.

Ion	Experimental <i>m/z</i>	Theoretical <i>m/z</i>	Δppm	Chemical formula
[Rolliniastatin-1-H+Cu <sup>II</sup> ] <sup>+</sup>	Internal standard	684.4021	-	C <sub>37</sub> H <sub>65</sub> O <sub>7</sub> Cu <sup>+</sup>
X <sub>3</sub>	573.3554	573.3575	-3.7	C <sub>31</sub> H <sub>58</sub> O <sub>5</sub> Cu <sup>+</sup>
Z <sub>3</sub>	544.3525	544.3547	-4.0	C <sub>30</sub> H <sub>57</sub> O <sub>4</sub> Cu <sup>+</sup>
C <sub>1</sub>	514.2334	514.2350	-3.1	C <sub>26</sub> H <sub>43</sub> O <sub>6</sub> Cu <sup>+</sup>
B <sub>1</sub>	471.2135	471.2166	-6.6	C <sub>24</sub> H <sub>40</sub> O <sub>5</sub> Cu <sup>+</sup>
C <sub>2</sub>	443.1843	443.1853	-2.3	C <sub>22</sub> H <sub>36</sub> O <sub>5</sub> Cu <sup>+</sup>
X <sub>2</sub>	403.1874	403.1904	-7.4	C <sub>20</sub> H <sub>36</sub> O <sub>4</sub> Cu <sup>+</sup>
Z <sub>2</sub>	374.1746	374.1877	-35.0*	C <sub>19</sub> H <sub>35</sub> O <sub>3</sub> Cu <sup>+</sup>
A <sub>2</sub>	373.1426	373.1435	-2.4	C <sub>18</sub> H <sub>30</sub> O <sub>4</sub> Cu <sup>+</sup>
X <sub>3</sub> -A <sub>2</sub>	263.1049	263.1067	-6.8	C <sub>12</sub> H <sub>24</sub> O <sub>2</sub> Cu <sup>+</sup>
Z <sub>2</sub> -C <sub>1</sub>	203.0113	203.0128	-7.4	C <sub>8</sub> H <sub>12</sub> O <sub>2</sub> Cu <sup>+</sup>

\* The low mass accuracy for this measurement is due to the presence of *m/z* 374.1468 which is an ion of the isotopic pattern of A<sub>2</sub>. When corrected considering this isotope, the theoretical *m/z* value of Z<sub>2</sub> is 374.1772 with Δppm = - 6.2.



**Scheme S1.** Proposed dissociation mechanism for Z<sub>2</sub> (purple arrows) fragment ion from [Rolliniastatin-1-H+Cu<sup>II</sup>]<sup>+</sup>.

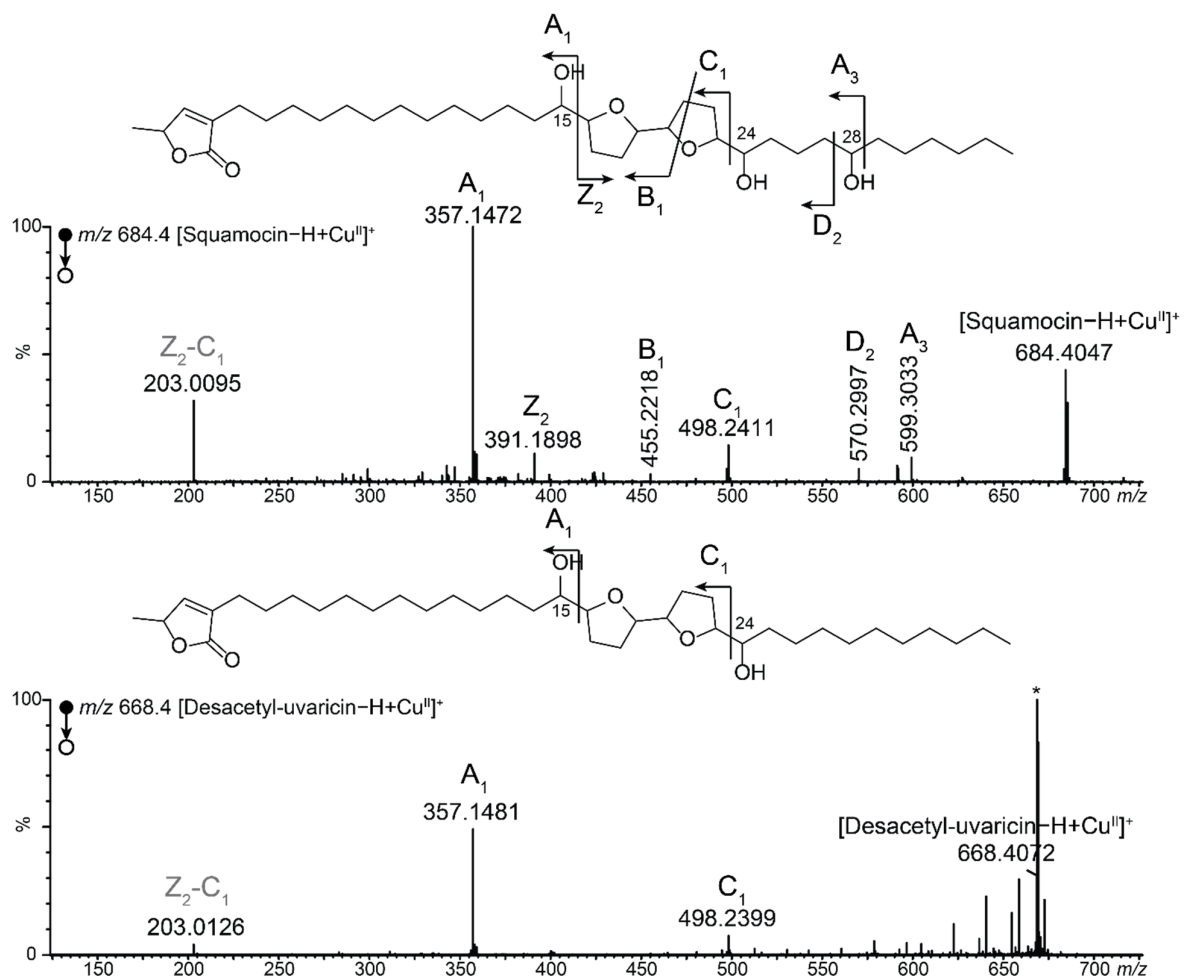


**Figure S5.** MS/MS spectra and the corresponding fragmentation scheme of a)  $[\text{Squamocin}-\text{H}+\text{Cu}^{\text{II}}]^+$  at 35 eV and b)  $[\text{Desacetyl-uvaricin}-\text{H}+\text{Cu}^{\text{II}}]^+$  at 10 eV from ESI-Q-TOF instrument.

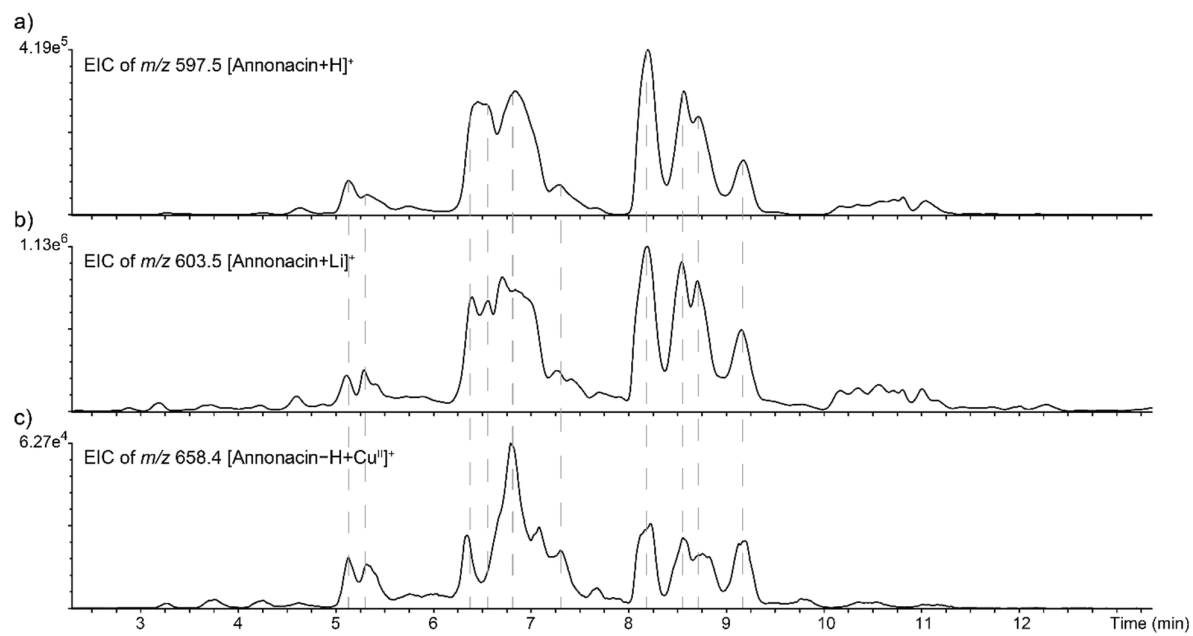


**Figure S6.** Extracted ion chromatogram of LC-MS spectra using in post-column infusion a) MeOH, b) MeOH with LiI at 10  $\mu$ M and c) MeOH with CuSO<sub>4</sub> at 1  $\mu$ M.

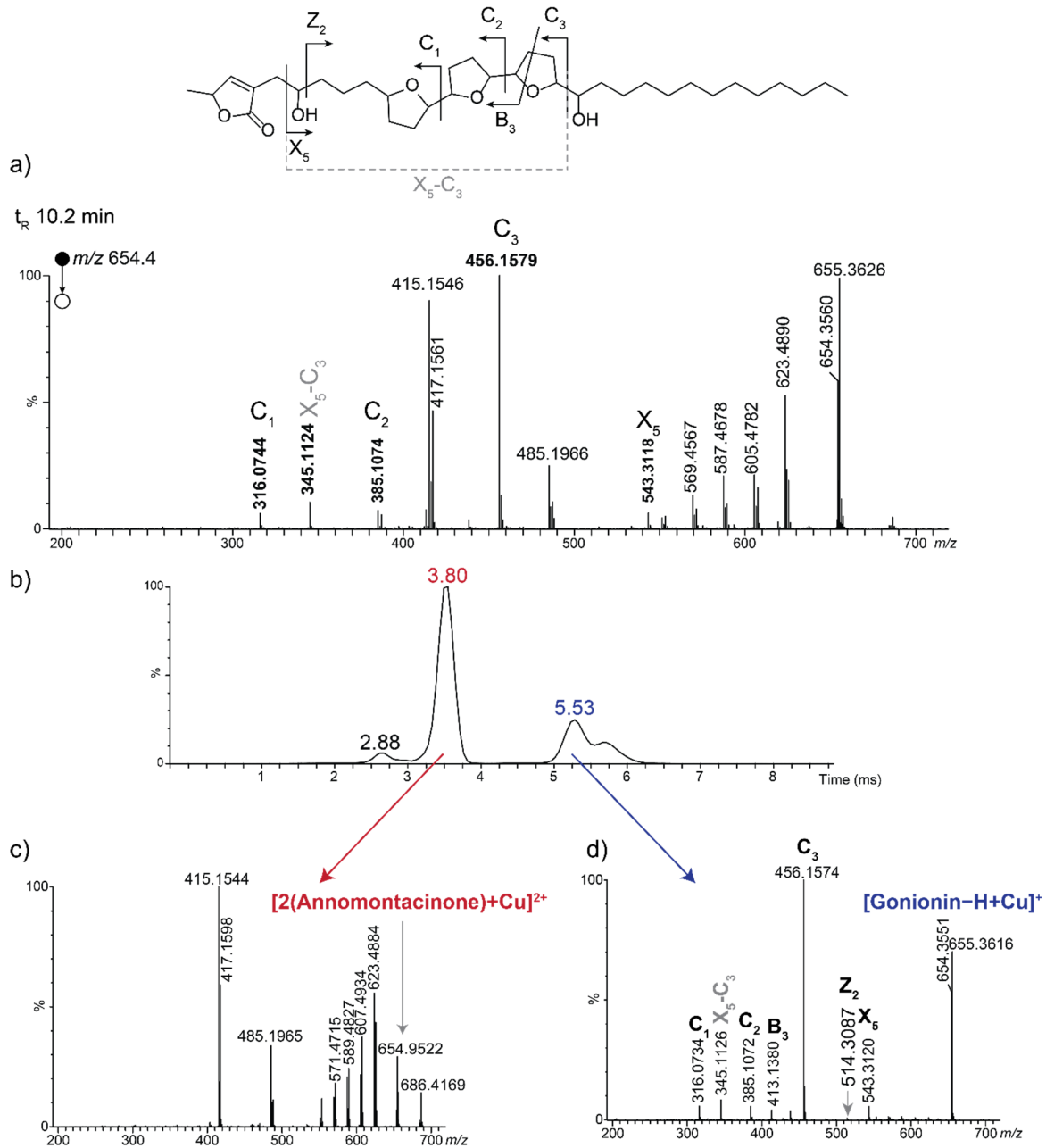


**Figure S7.** MS/MS spectra from LC-IMS-MS/MS experiments a) without using the IMS dimension, and after IMS differentiation of c)  $[2(\text{annomontacinone}+\text{Cu})^{2+}]$  ( $m/z$  654.4468) vs d)  $[\text{Gonionin}-\text{H}+\text{Cu}]^+$  ( $m/z$  654.3551) from the b) extracted IMS spectrum of the corresponded  $t_R$ .

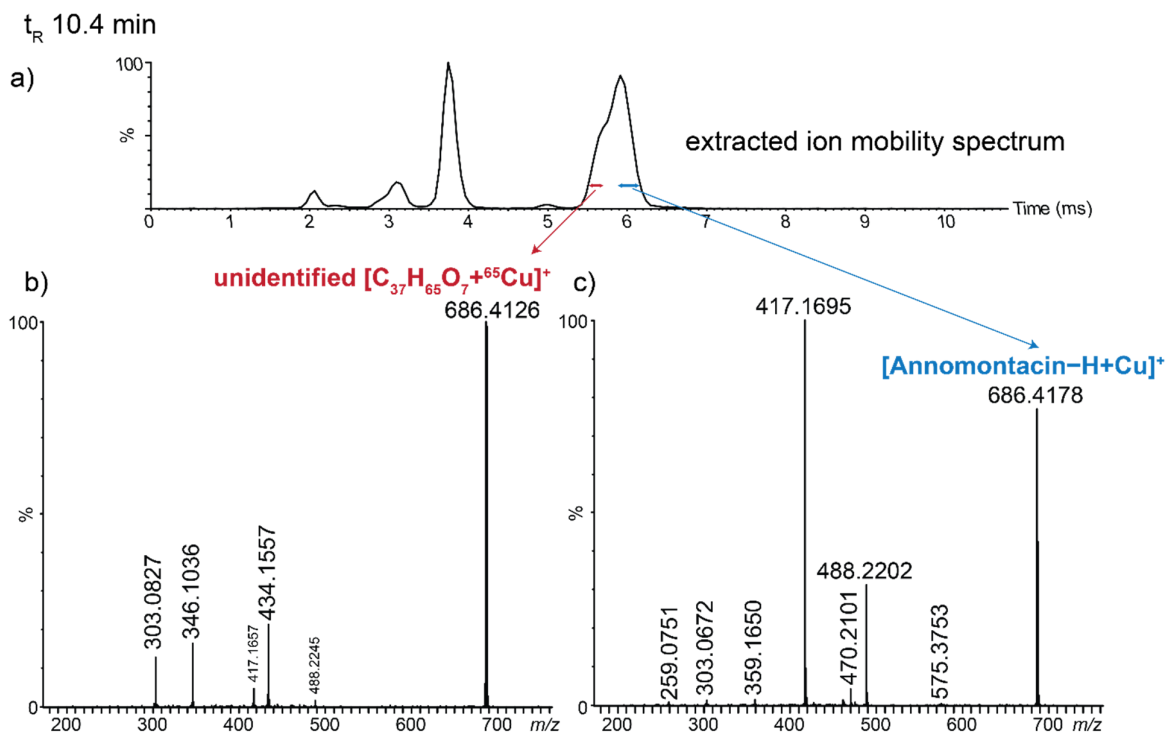


**Figure S8.** a) Extracted ion mobility spectrum of  $t_R$  10.2 min from LC-IMS-MS/MS of  $m/z$  686.4 and extracted MS/MS spectra of b) left part of the ion mobility peak corresponding to  $[C_{37}H_{65}O_7 + ^{65}Cu]^+$ , which was not attributed and c) right part of the ion mobility peak corresponding to  $[Annomontacin-H + ^{63}Cu]^+$ .

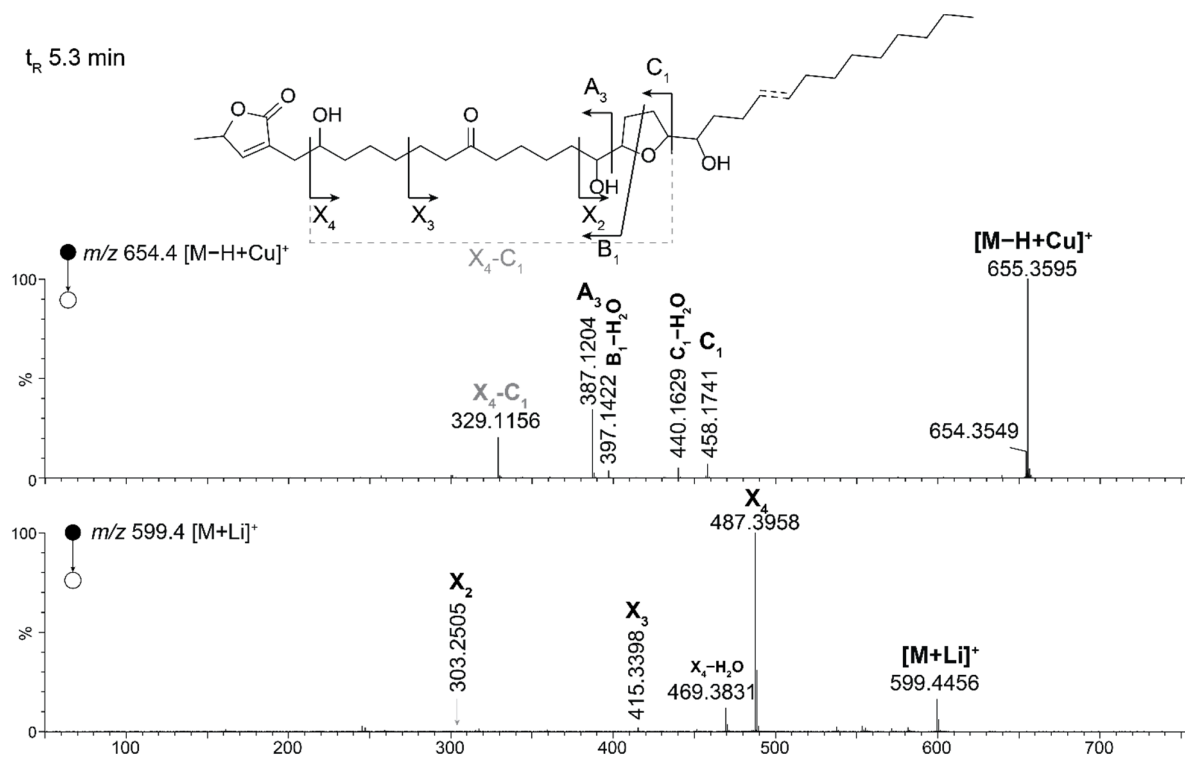


**Figure S9.** MS/MS spectra of  $[M1-H+Cu^{II}]^{+}$  at 20 eV (top) and of  $[M1+Li]^{+}$  at 65 eV (bottom) from LC-ESI-QTOF-MS/MS experiments and the corresponding fragmentation scheme.

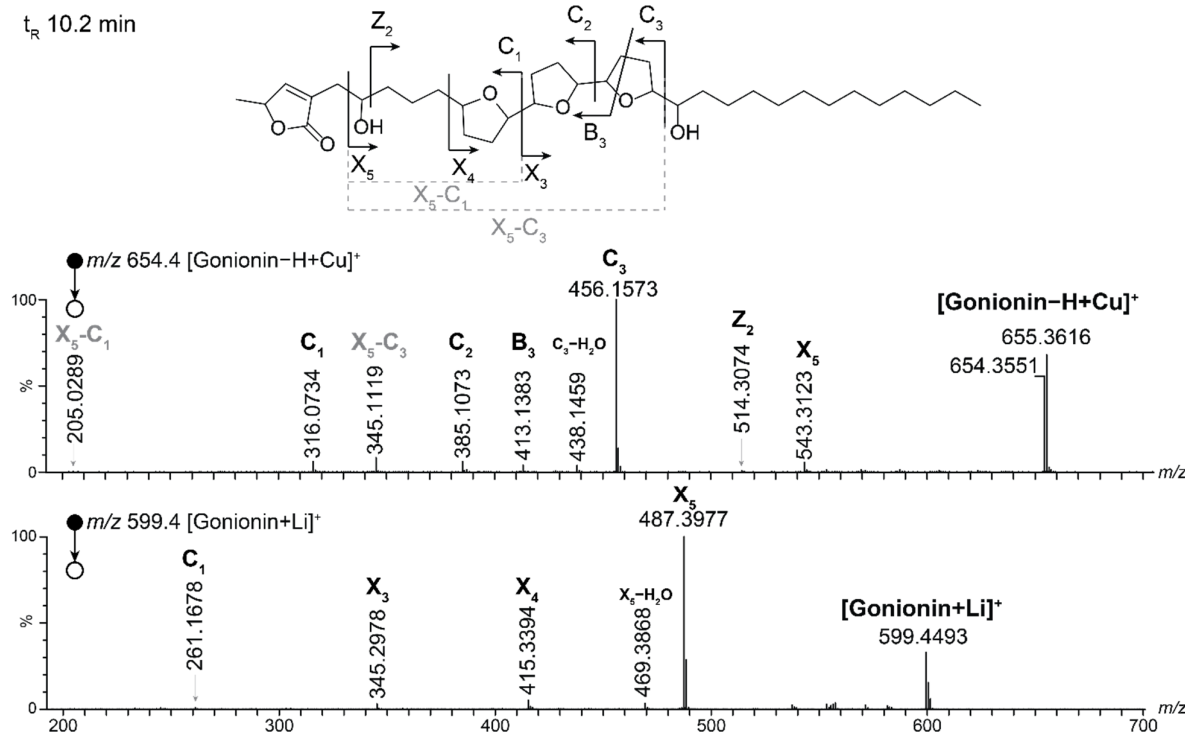


**Figure S10.** MS/MS spectra of  $[Goniodonin-H+Cu^{II}]^{+}$  at 20 eV (top) and of  $[Goniodonin+Li]^{+}$  at 65 eV (bottom) from LC-ESI-QTOF-MS/MS experiments and the corresponding fragmentation scheme.

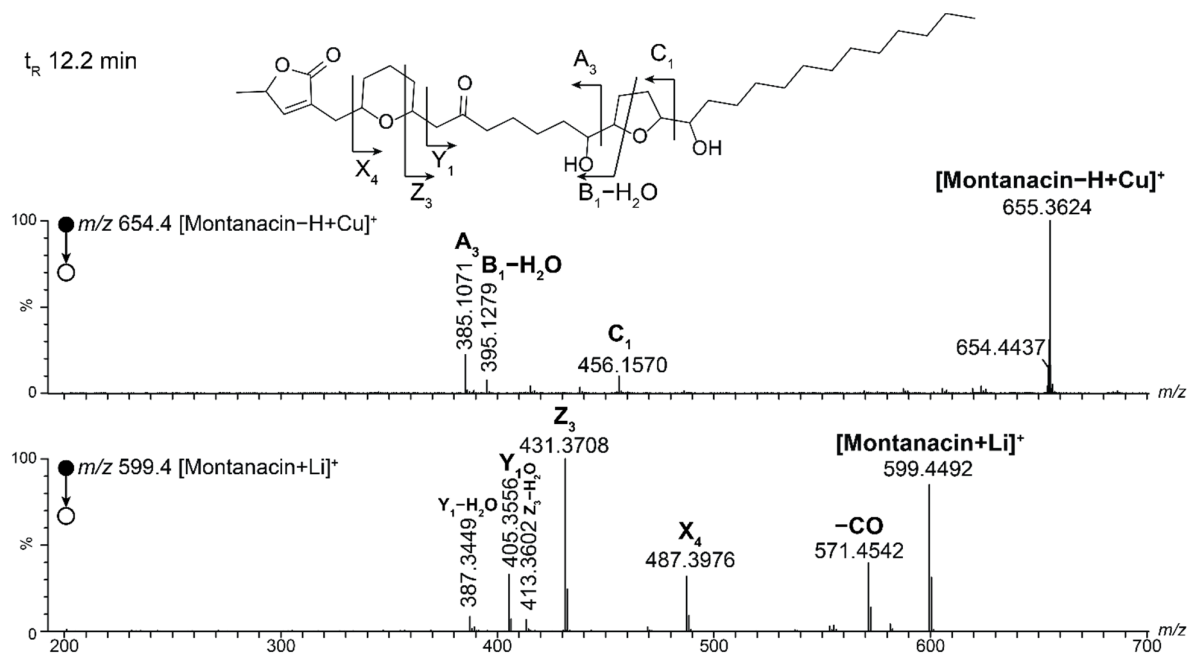


**Figure S11.** MS/MS spectra of  $[\text{Montanacin-D-H}+\text{Cu}^{II}]^+$  at 20 eV (top) and of  $[\text{Montanacin-D+Li}]^+$  at 65 eV (bottom) from LC-ESI-QTOF-MS/MS experiments and the corresponding fragmentation scheme.

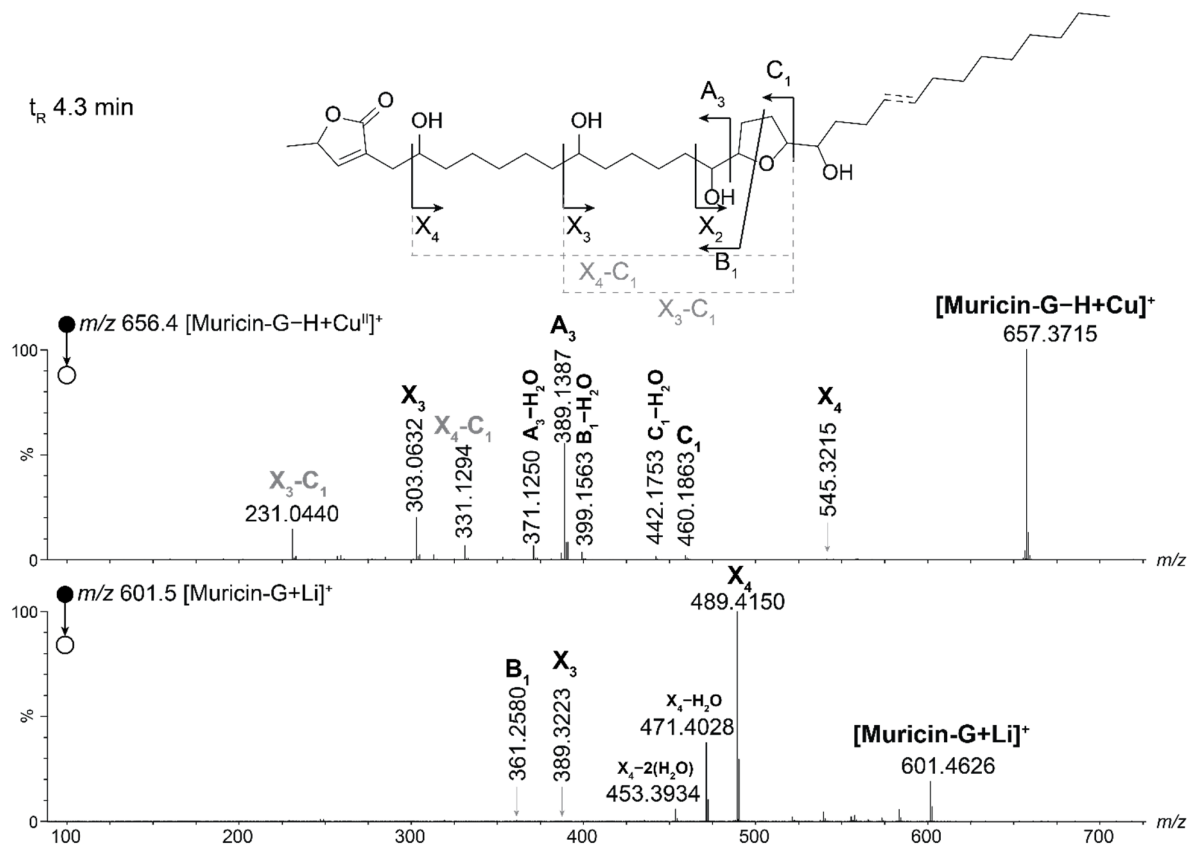


**Figure S12.** MS/MS spectra of  $[\text{Muricin-G-H}+\text{Cu}^{II}]^+$  at 20 eV (top) and of  $[\text{Muricin-G+Li}]^+$  at 65 eV (bottom) from LC-ESI-QTOF-MS/MS experiments and the corresponding fragmentation scheme.

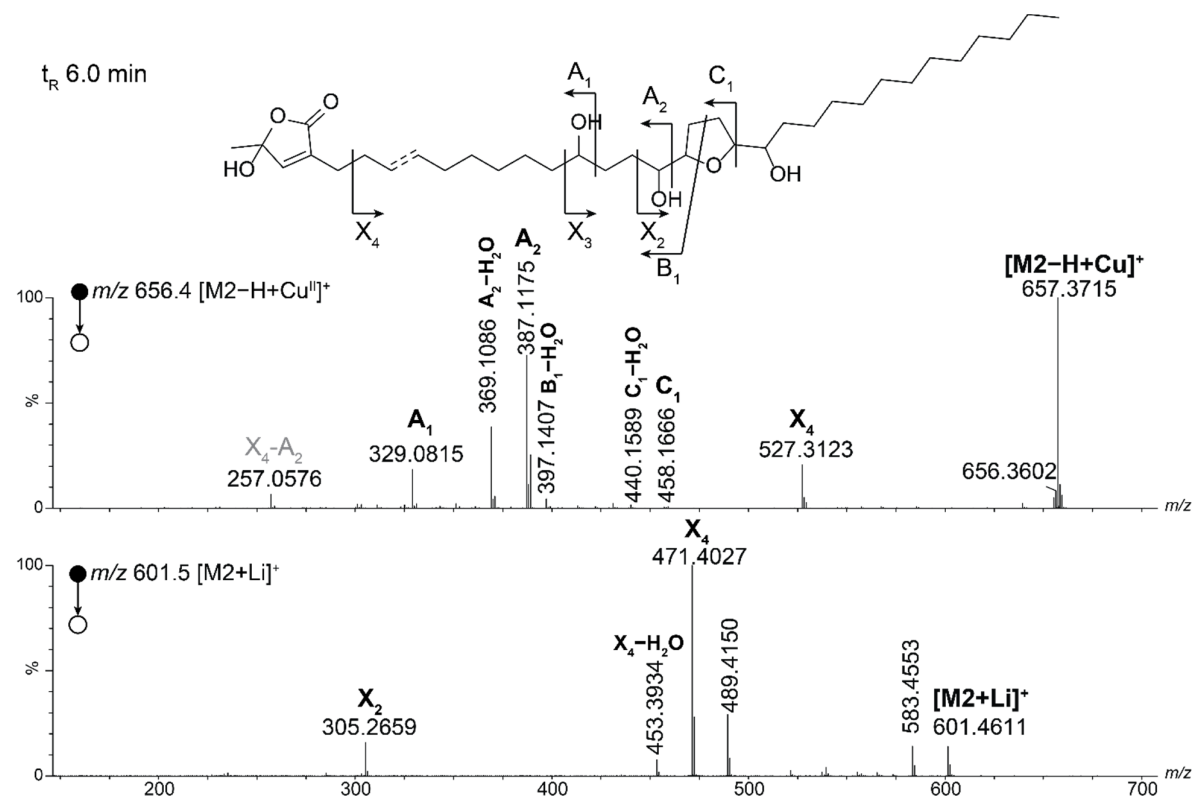


**Figure S13.** MS/MS spectra of  $[M2-H+Cu^{II}]^+$  at 20 eV (top) and of  $[M2+Li]^+$  at 65 eV (bottom) from LC-ESI-QTOF-MS/MS experiments and the corresponding fragmentation scheme.

$t_R$  10.4 min

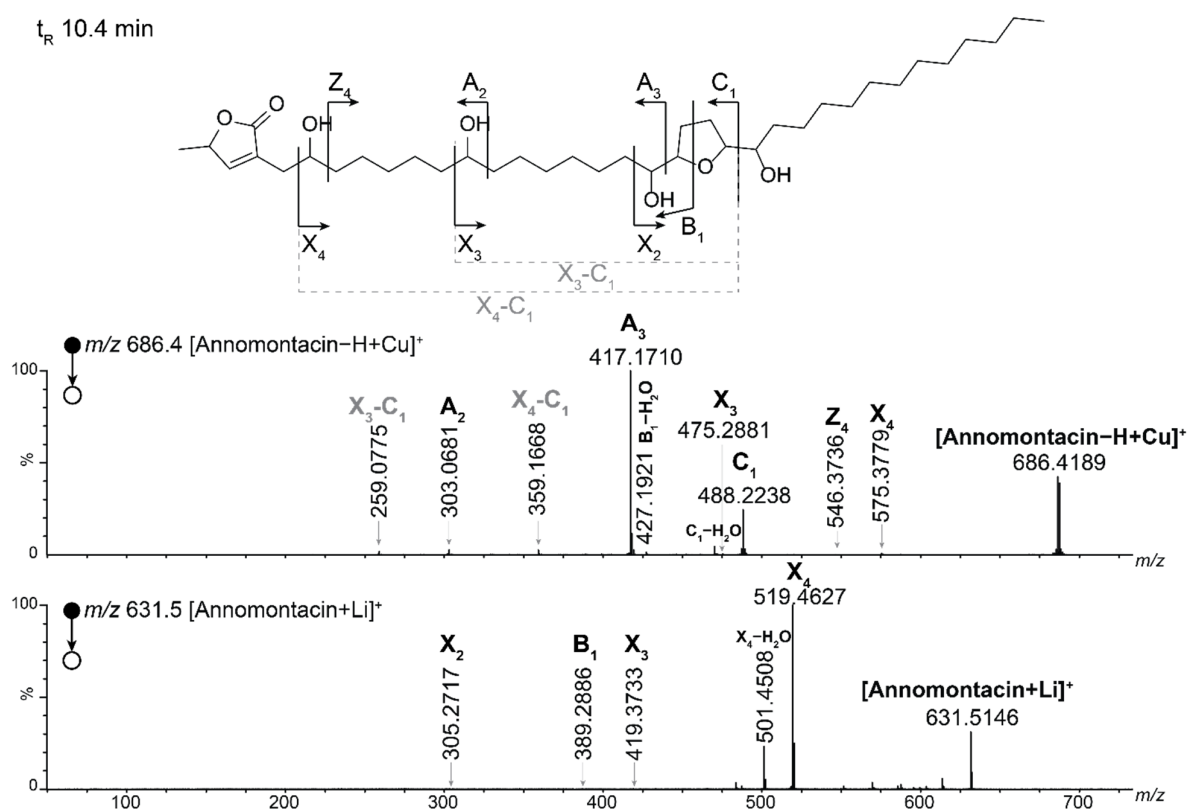


**Figure S14.** MS/MS spectra of  $[\text{Annomontacin}-\text{H}+\text{Cu}^{\text{II}}]^+$  at 20 eV (top) and of  $[\text{Annomontacin}+\text{Li}]^+$  at 65 eV (bottom) from LC-ESI-QTOF-MS/MS experiments and the corresponding fragmentation scheme.

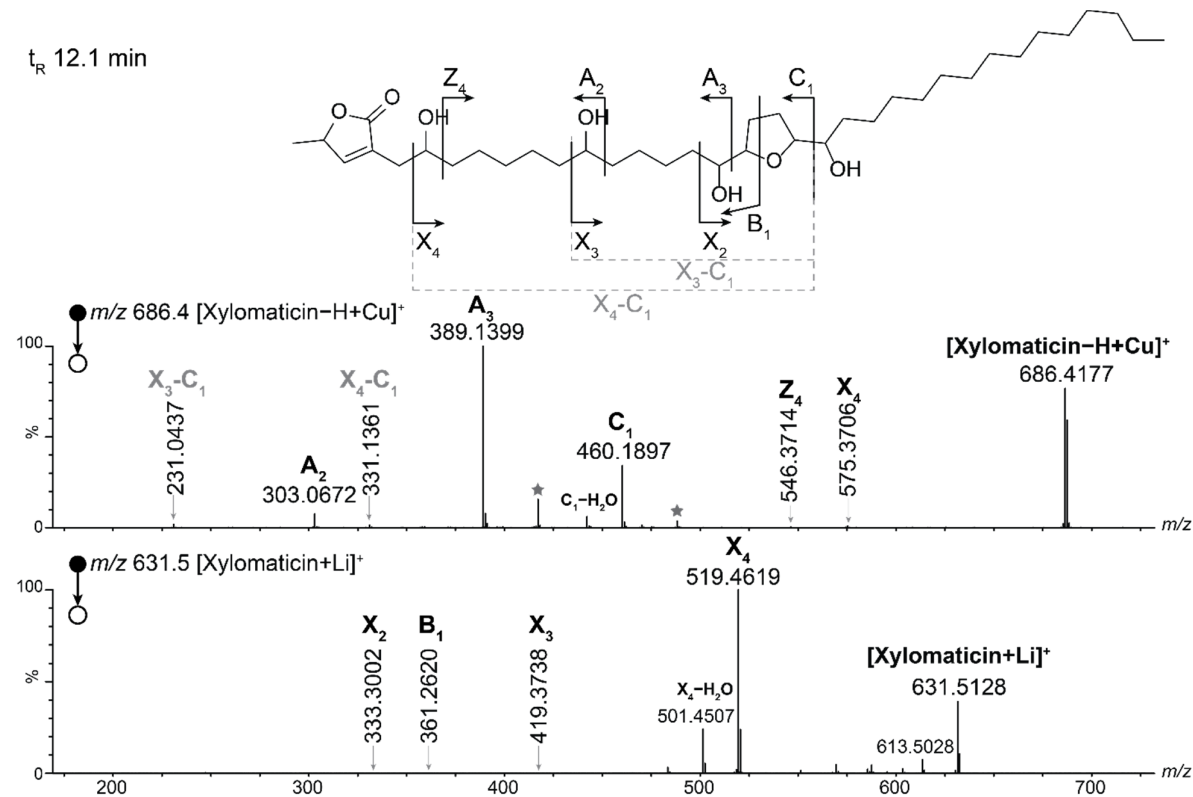


**Figure S15.** MS/MS spectra of  $[Xylomaticin-H+Cu^{II}]^{+}$  at 20 eV (top) and of  $[Xylomaticin+Li]^{+}$  at 65 eV (bottom) from LC-ESI-QTOF-MS/MS experiments and the corresponding fragmentation scheme.

Signal annotated with a star corresponds to the isotope  $^{65}\text{Cu}$  of Annomontacin-10-one observed at the same  $t_R$ .

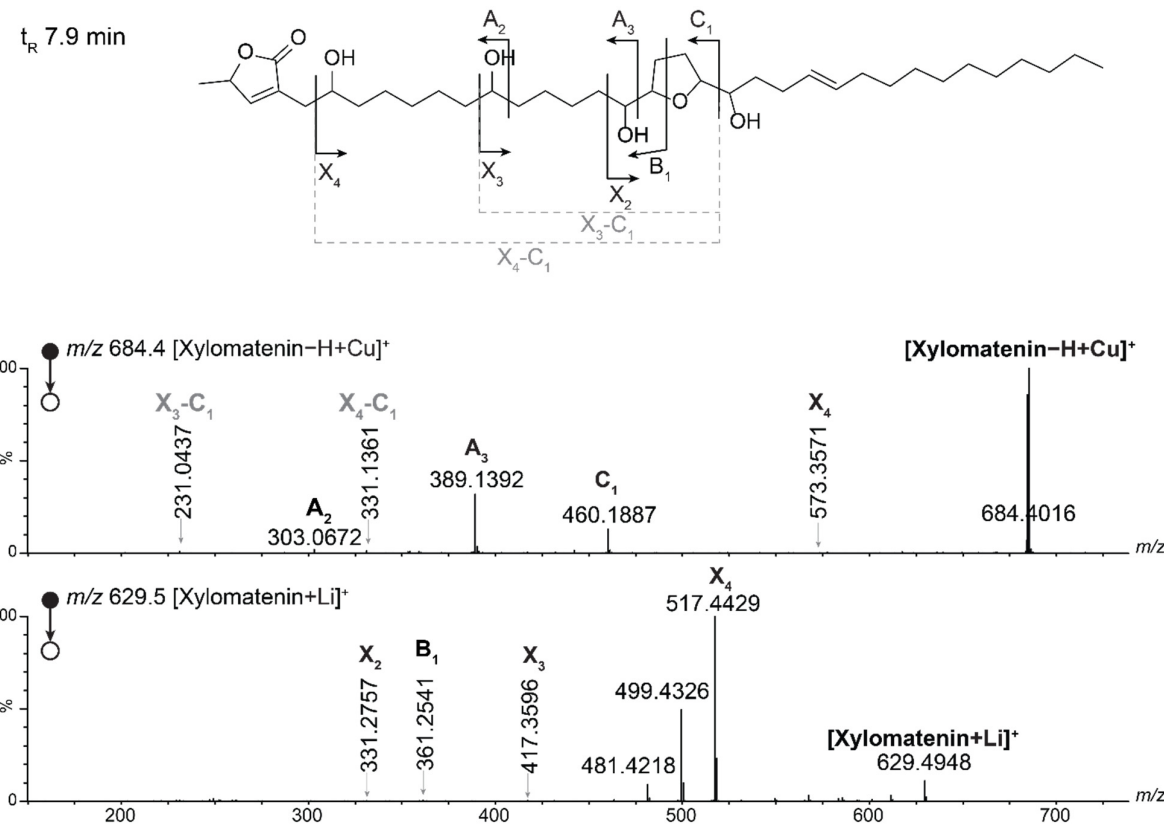


**Figure S16.** MS/MS spectra of  $[\text{Xylomatenin}-\text{H}+\text{Cu}^{\text{II}}]^+$  at 20 eV (top) and of  $[\text{Xylomatenin}+\text{Li}]^+$  at 65 eV (bottom) from LC-ESI-QTOF-MS/MS experiments and the corresponding fragmentation scheme.

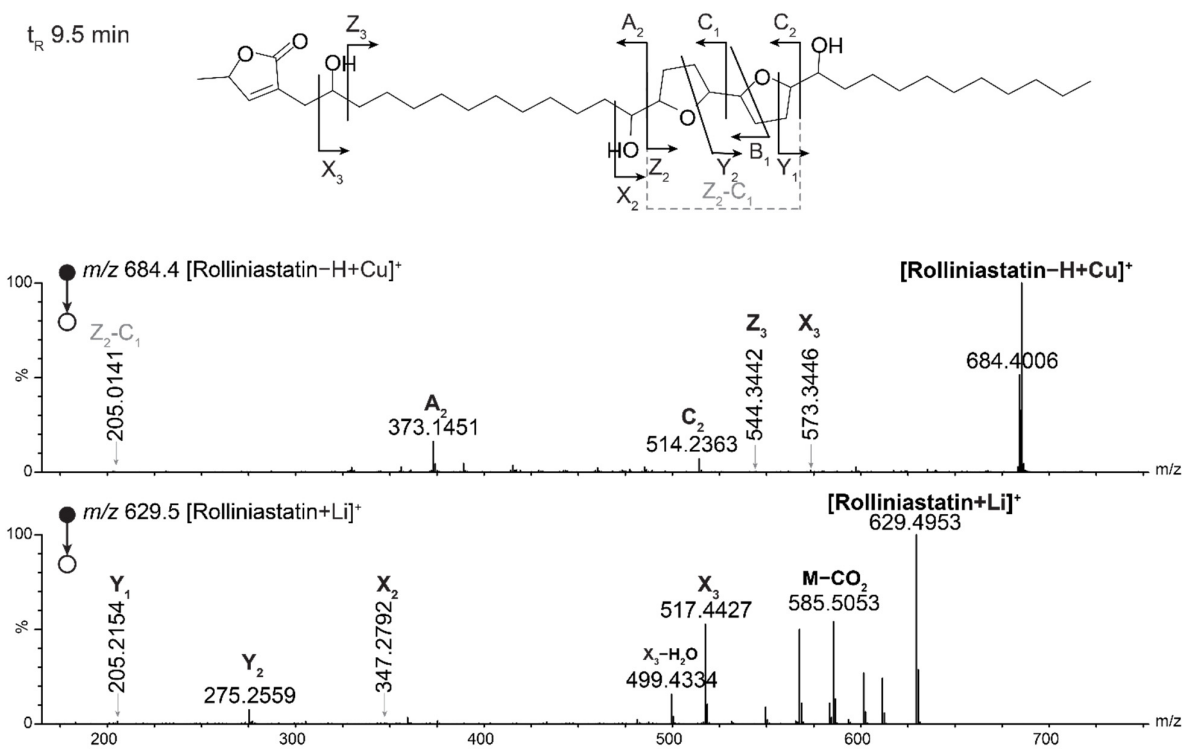


**Figure S17.** MS/MS spectra of  $[\text{Rolliniastatin}-\text{H}+\text{Cu}^{\text{II}}]^+$  at 20 eV (top) and of  $[\text{Rolliniastatin}+\text{Li}]^+$  at 65 eV (bottom) from LC-ESI-QTOF-MS/MS experiments and the corresponding fragmentation scheme.

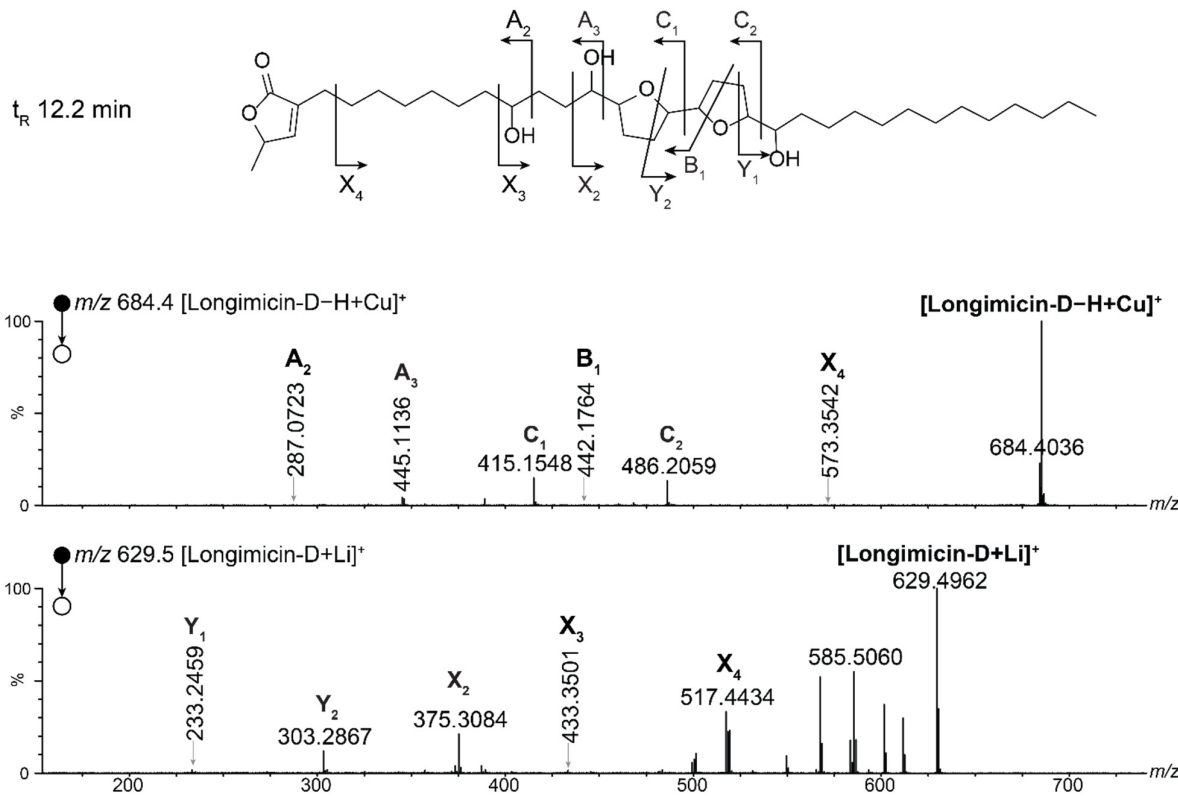


**Figure S18.** MS/MS spectra of  $[\text{Longimicin-D}-\text{H}+\text{Cu}^{\text{II}}]^+$  at 20 eV (top) and of  $[\text{Longimicin-D}-\text{Li}]^+$  at 65 eV (bottom) from LC-ESI-QTOF-MS/MS experiments and the corresponding fragmentation scheme.

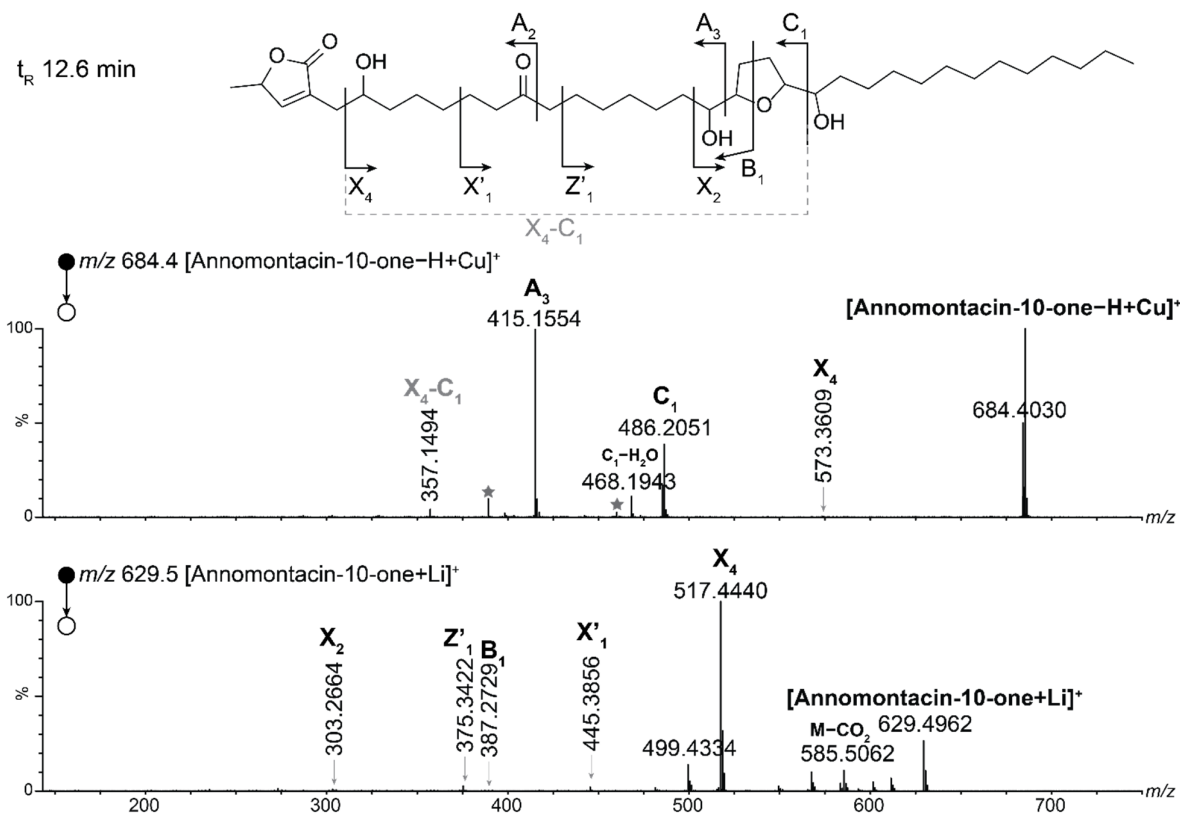


**Figure S19.** MS/MS spectra of [Annomontacin-10-one-H+Cu<sup>II</sup>]<sup>+</sup> at 20 eV (top) and of [Annomontacin-10-one+Li]<sup>+</sup> at 65 eV (bottom) from LC-ESI-QTOF-MS/MS experiments and the corresponding fragmentation scheme.

**Table S4.** Identified analogues from LC-MS/MS experiments of [acetogenins-H+Cu<sup>II</sup>]<sup>+</sup>

<i>m/z</i>	ID	Oxygen cycle	OH	CO	DB	Name
654.3526	2	16-19	4, 15, 20	10	[21-33]	
		8-11,12-15,16-19	4, 20			Gonionin
		4-8, 16-19	15, 20	10		Montanacin D <sup>a</sup>
656.3641	78, 81, 85	16-19	4,10,15,20		[21-33]	Muricin G <sup>b</sup>
	79	16-19	12,15,20,34		[3-11]	
	76, 77, 80, 83	16-19	4, 15, 20	10		Annonacinone <sup>a</sup>
	75, 87	12-15, 16-19	4, 11, 20			Longimicin B
	89	10-13, 16-19	4, 15, 20			
658.3829	102	16-19	10,15,20,34			
	93, 95	16-19	4,10,15,20			Annonacin <sup>a</sup>
		16-19	4,8,15,20			Xylopiandin <sup>a</sup>
	94	16-19	4,12,15,20			Glacin B
	92, 99	10-13	4,14,17,18			Gigantetrocin A
	90, 91	14-17	4,10,13,18			Goniothalamicin <sup>a</sup>
672.3681	17, 20	16-19	4,12,15,20	10		
	10	16-19	4,15,20,34	10		Goniodoninone
674.3817	37, 41	16-19	4,10,14,15,20			
	35	16-19	4,10,13,15,20			
	33, 36, 38	16-19	4,10,11,15,20			Annomuricin B
	34	16-19	4,10,15,20,34			Goniodonin <sup>a</sup>
		16-19	4,10,15-20		[21-35]	Xylomatenin <sup>b</sup>
684.4047		16-19, 20-23	4, 15, 24			Rolliniastatin
	24	18-21	4, 17, 22	12		Annomontacin-12-one
	23, 25	10-13	4,14,17,18		[19-35]	Gigantetronenin <sup>c</sup>
	26, 27	18-21	4, 17, 22	10		Annomontacin-10-one
		14-17, 18-21	10, 13, 22			Longimicin D
	31, 32	14-17, 18-21	[4-12],13,22			
	28	10-13, 18-21	14, 17, 22			4-deoxygigantecin
	61, 62, 63	18-21	4,10,17,22			Annomontacin
686.4210	60, 64	16-19	4,10,15,20			Xylomaticin
	41	16-20	4,10,14,15,20			
700.3977	46, 47	14-17, 18-21	4,10,13,22			10-Hydroxyglaucanetin
	45	10-13, 18-21	4,14,17,22			Gigantecin

Grey entries were not observed on the molecular network as they were identified after IMS separation from isobars.

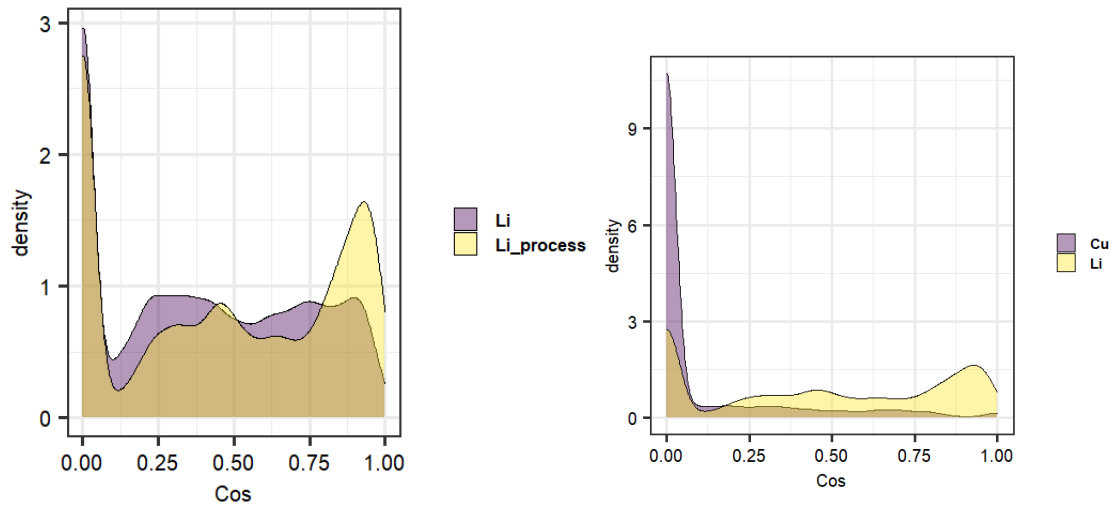


**Figure S20.** Cosine score plots of a) Li molecular network (MN) with a 14 Da window limit in purple vs Li MN with 100 Da window limit in yellow and b) comparison between Li MN in yellow and Cu MN in purple

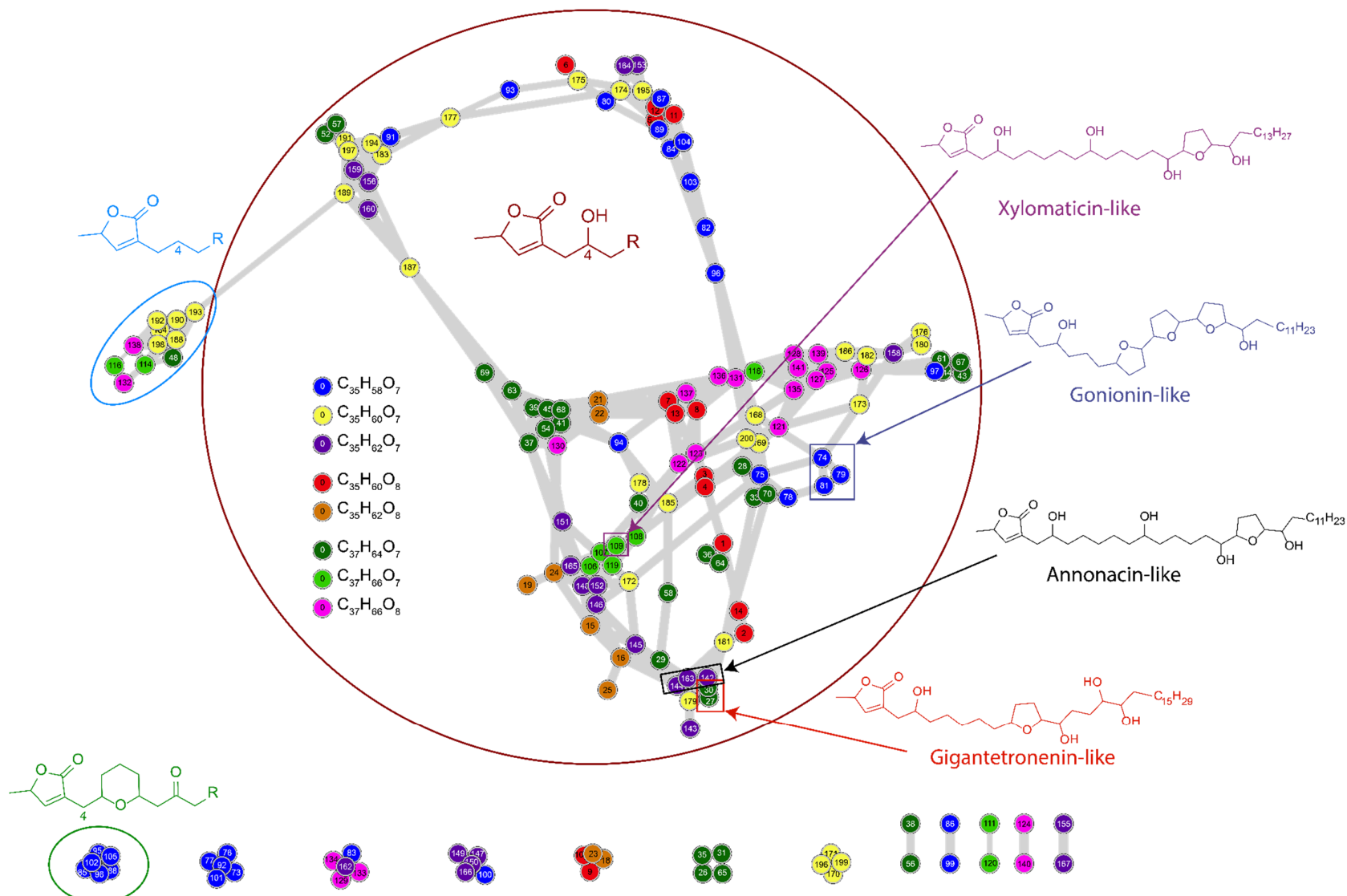


**Figure S21.** Molecular network of 8 lithiated precursor ions from an *Annona muricata* extract. Nodes colors are based on the  $m/z$  of the precursor ion as followed: 599.45 in blue, 601.46 in yellow, 603.48 in purple, 617.46 in red, 619.47 in orange, 629.49 in dark green, 631.52 in pale green and 645.49 in pink.